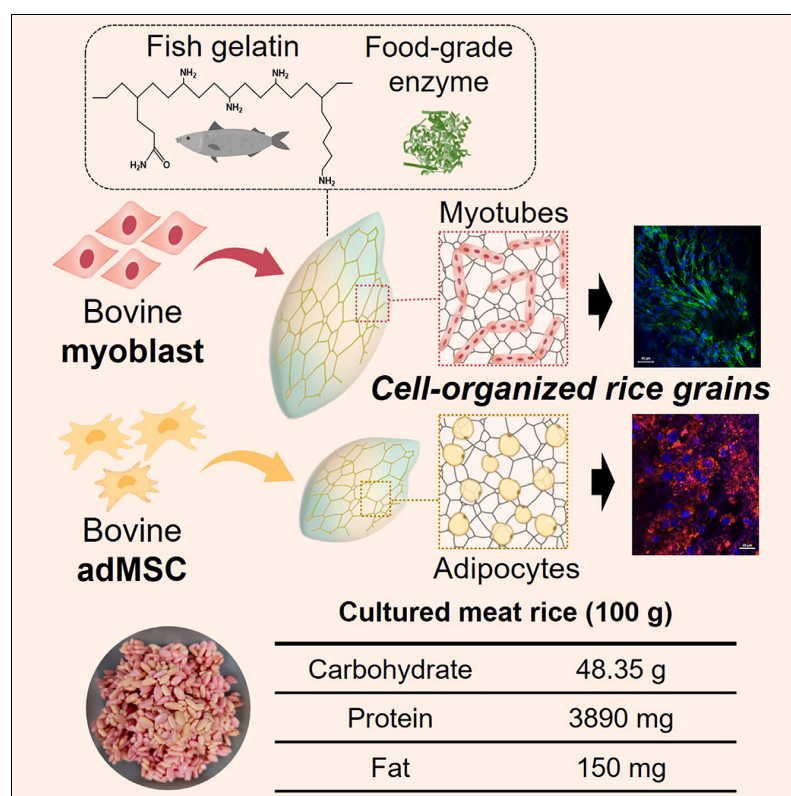


## Article

# Rice grains integrated with animal cells: A shortcut to a sustainable food system

Pdf by:  
<https://www.pro-memoria.info>



A novel food ingredient that can overcome humanity's food crisis has been created. Rice grains, a common food ingredient, are coated with gelatin and food enzymes to become a home for cells that can contain many animal cells. Bovine muscle cells and fat cells grow and organize on the surface and inside the rice grain. This product is reminiscent of microbeef sushi and has a different texture, nutritional profile, and flavor than traditional rice grains.

Sohyeon Park, Milae Lee, Sungwon Jung, ..., Heeyoun Hwang, Sangmin Lee, Jinkee Hong

slee98@cau.ac.kr (S.L.)  
 jinkee.hong@yonsei.ac.kr (J.H.)

### Highlights

Rice grains coated with fish gelatin/enzymes have improved structural stability

Coated rice grains serve as a nutritious scaffold for the organization of cells

Bovine-cell-organized grains with rice grains and animal cells are developed

Food properties of cell-organized rice show its potential as a future food element



## Development

Practical, real world, technological considerations and constraints

Park et al., Matter 7, 1–22  
 March 6, 2024 © 2024 Elsevier Inc.  
<https://doi.org/10.1016/j.matt.2024.01.015>

Article

# Rice grains integrated with animal cells: A shortcut to a sustainable food system

Sohyeon Park,<sup>1</sup> Milae Lee,<sup>1</sup> Sungwon Jung,<sup>1</sup> Hyun Lee,<sup>2</sup> Bumgyu Choi,<sup>1</sup> Moonhyun Choi,<sup>1</sup> Jeong Min Lee,<sup>2</sup> Ki Hyun Yoo,<sup>3</sup> Dongoh Han,<sup>3</sup> Seung Tae Lee,<sup>2</sup> Won-Gun Koh,<sup>1</sup> Geul Bang,<sup>4</sup> Heeyoun Hwang,<sup>4,5</sup> Sangmin Lee,<sup>6,\*</sup> and Jinkee Hong<sup>1,7,\*</sup>

## SUMMARY

**A strategy to develop a nutrient-rich hybrid food using rice grains functionalized with nanocoating and bovine cells for a sustainable food system is reported. Rice grains are safe food ingredients with a low incidence of allergy and have a nutritional profile and structure suited for 3D cell culture. An edible coating composed of fish gelatin and food enzymes offers a high affinity between rice grains and cells and improves the structural stability of grains for increased cell capacity. The potential of rice grains as cell scaffolds is demonstrated by investigating the interactions between the coating, grains, and cells. The rice grains are transformed into a hybrid food with animal nutrients by containing organized bovine cells. We discuss the food properties and production value of this rice-based meat to evaluate its potential as a sustainable food that guarantees safety from food crises and global warming.**

## INTRODUCTION

As the concept of sustainable development gains popularity, future food development is emphasized.<sup>1,2</sup> Due to external factors, such as rising health concerns, infectious disease risks, climate change, and resource scarcity, the food system is undergoing structural changes.<sup>3–6</sup> Securing a stable food system against the unavoidable food crisis is a long-cherished business of mankind today.<sup>2,7</sup> The vegan market continues to expand, and numerous future food ingredients are proposed. According to reports, fascinating future foods include synthetic meats, algae, insect-derived proteins, genetically modified (GM) foods, and 3D-printed foods.<sup>8</sup> To achieve a sustainable food system, the production process of food ingredients should be safe and stable, and manufactured foods should have even nutrients and excellent processability.<sup>9,10</sup> Unfortunately, the future food candidates reported so far have practical limitations in terms of commercialization, such as nutritional imbalance, unfamiliar taste, poor formability, and price competitiveness.

In this context, hybrid foods formed from the combination of vegetable and animal ingredients have tremendous potential to grow into reasonable future foods.<sup>11–13</sup> A typical example of hybrid protein food is cell-cultured meat using a soy or nut-based scaffold, such as textured vegetable protein (TVP).<sup>14,15</sup> It is worth noting that TVP-based cultured meat is sold in Singapore. Additionally, interesting scaffolds such as eggshell membrane-based microcarriers,<sup>16</sup> 3D-printed Prolamin scaffolds,<sup>17</sup> and gellan gum-gelatin scaffolds<sup>18</sup> have been used recently to develop hybrid meat. However, scaffolds based on soy and nut ingredients are typical allergens. Moreover, the acceptable cellular content of these scaffolds is low, resulting in

## PROGRESS AND POTENTIAL

The development of future food is an inevitable task for sustainable humanity. Unfortunately, the future food candidates reported so far have practical limitations in terms of commercialization, such as nutritional imbalance, unfamiliar taste, and poor formability. Accordingly, this study proposes to develop a new food ingredient in which rice grains, nanocoating, and animal cells are integrated. The food properties and value of these rice-based meats are discussed, assessing their potential as sustainable food ingredients. The findings of this study provide feasible ideas for creating various types of future hybrid foods. In the future, this self-production system of grain-based hybrid foods could ensure food relief in underdeveloped countries, during war, and in space.

excess additives being used to flavor the meat. Coating the scaffold with mammal-derived proteins or extending the cell culture period is sometimes adopted to increase cell content in hybrid meat.

Rice grains contain carbohydrates, fats, and proteins as well as minerals such as phosphorus, calcium, and magnesium.<sup>19–21</sup> They also contain functional ingredients, such as glutelin and folic acid, that play a crucial role in the cellular metabolic activities of skeletal muscle cells, thereby promoting normal cell development and slowing aging.<sup>21,22</sup> It is worth noting that rice grains are safe ingredients that are far from being allergenic. In a cell culture environment, the rice grain itself can nourish cells and promote their proliferation. For example, selenium in rice grains regulates redox and is directly involved in the cell cycle of mammalian cells.<sup>22,23</sup> The blocklet packing structure of the rice grain provides a large surface area as well as a porous and organized volume, allowing animal-derived cells to reside.<sup>24,25</sup> In addition, the crystalline and semi-crystalline cross-structures of the grains could guide the adhesion and growth of cells in a particular direction. From the perspective of hybrid food, these nutritional and structural characteristics of rice grains indicate their great potential as 3D cell scaffolds.

In this study, rice grains containing bovine cells are proposed as a novel food ingredient for a sustainable food system. The rice grains were functionalized with an edible coating consisting of fish gelatin and food-grade enzymes to maximize their cell capacity. We used fish gelatin, a non-mammalian material closest to the extracellular matrix (ECM), but various eco-friendly ingredients with high cell affinity can be used as a coating material. The edible coatings enhance the cell adhesion and structural stability of rice grains, supporting them to serve as durable 3D scaffolds during cell culture. Through this strategy, it is possible to develop a safe and practical hybrid food in which food, scaffold, and cells are mutually beneficial. Bovine myoblasts and adipose tissue-derived mesenchymal stem cells (adMSCs) proliferated and differentiated on the coated grains to synthesize nutrient-dense grains containing organized cells. We discuss the food properties and production value, including CO<sub>2</sub> emission reduction, nutritional value, and production process, of this rice-based meat to evaluate its potential as a sustainable food ingredient. The strategy and findings of this study provide feasible ideas for the development of various types of cell-based future foods. As this technology is applicable to a food system capable of self-development, these hybrid grains can be developed as relief food in response to emergencies and in underdeveloped countries, during war, and in space (Figure 1).

## RESULTS

### Functionalization of rice grains using food-graded gelatin and enzymes

Most grains, including rice grains, have a granular structure. Rice grains are made up of about 80% starch, 20% protein, and other minerals; rice starch is closely related to the physicochemical properties of the rice grains. We applied an edible coating on the rice grains to modify their physicochemical factors associated with cell uptake to create granular structures capable of holding many cells. The structure of rice grains consists of semi-crystalline and amorphous starch growth rings, amorphous channels, and a hard crystalline shell.<sup>25</sup> The semi-crystalline lamellae of the growth rings consist of packed amylopectin and amylose. Amylopectin is a crystalline region with an ordered double-helix structure, whereas amylose occupies an amorphous region of a single-helix structure stabilized by hydrogen bonds.<sup>26</sup>

For the functionalization of rice grains, we used fish gelatin and microbial transglutaminase (mTG) as coating materials. To reduce resource consumption and

---

<sup>1</sup>Department of Chemical & Biomolecular Engineering, College of Engineering, Yonsei University, 50 Yonsei-ro, Seodaemun-gu, Seoul 03722, Republic of Korea

<sup>2</sup>Department of Applied Animal Science, Kangwon National University, 1 Kangwondaehak-gil, Chuncheon-si, Gangwon-do 24341, Republic of Korea

<sup>3</sup>Simple Planet, Inc., 34, Sangwon 12-gil, Seongdong-gu, Seoul 04790, Republic of Korea

<sup>4</sup>Digital OMICs Research Center, Korea Basic Science Institute, 162 Yeongudanji-ro, Cheongju-si, Chungbuk 28119, Republic of Korea

<sup>5</sup>Critical Diseases Diagnostics Convergence Research Center, Korea Research Institute of Bioscience and Biotechnology, 125 Gwahak-ro, Yuseong-gu, Daejeon, 34141, Republic of Korea

<sup>6</sup>School of Mechanical Engineering, Chung-Ang University, 84 Heukseuk-ro, Dongjak-gu, Seoul 06974, Republic of Korea

<sup>7</sup>Lead contact

\*Correspondence: [slee98@cau.ac.kr](mailto:slee98@cau.ac.kr) (S.L.), [jinkee.hong@yonsei.ac.kr](mailto:jinkee.hong@yonsei.ac.kr) (J.H.)

<https://doi.org/10.1016/j.matt.2024.01.015>

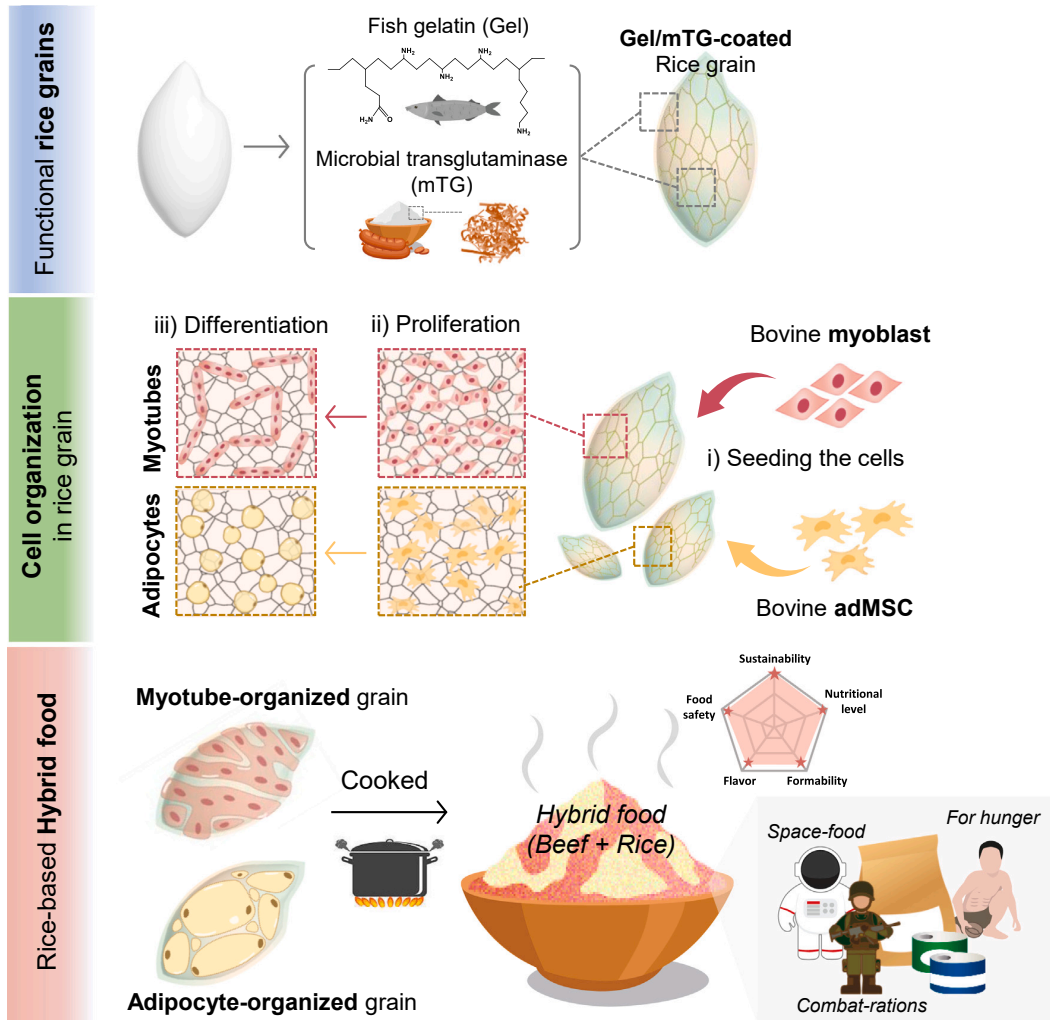


**Figure 1. A schematic showing the synthesis process of hybrid rice integrated with bovine cells using bovine cells and Gel/mTG coating-functionalized rice grains**

The food benefits and application values of the developed hybrid rice grains are described.

environmental problems caused by raising livestock, fish gelatin rather than mammalian gelatin was used as a coating material in this experiment. Fish gelatin is less expensive than mammalian gelatin but exhibits poor thermal stability and mechanical properties. We accordingly chose mTG, which is utilized in the production of dairy and bakery products as well as the processing of meat, as an additional coating material. mTG is a well-known food additive enzyme that effectively cross-links glutamine and lysine in gelatin.<sup>27,28</sup> We anticipated that the gelatin/mTG (Gel/mTG) coating would enhance the chemical and physical stability of the rice grains by binding to them and delivering the RGD sequence. Starch and gelatin can form hydrogen bonds, and the gelatin chains bound to starch are crosslinked by mTG.

We analyzed Raman spectra to elucidate the successful formation of coated rice grains. Raman spectroscopy is an analysis tool often used to inspect the quality of rice grains, such as changes in the content of amylose and amylopectin depending

on the grain's origin and storage period. The overall Raman spectrum was subdivided into starch C–O–C, polysaccharide, and amide bond regions. The glucose ring-stretching peak at  $478\text{ cm}^{-1}$  was used as a standard to normalize the overall spectrum of the three regions because it exhibits a constant shape and negligible frequency shifts for different rice samples (Figure 2).<sup>29</sup> Full width at half maximum (FWHM) of the starch C–O–C peak, corresponding to the glucose ring-stretching peak, reflects the starch short-range-ordered structure in the starch C–O–C region. The higher the FWHM, the less ordered the short-range structure.<sup>30</sup> As depicted in Figure 2B, the C–O–C peak FWHMs of the bare and coated grains are 16.965 and 16.781, respectively, which are nearly identical, indicating that the Gel/mTG coating did not significantly affect the decomposition and alignment of the rice starch. In addition to the C–O–C bending peak, coated rice grains exhibited an increased peak near  $1,000\text{ cm}^{-1}$  in the polysaccharide region. This peak indicates the presence of the protein constituent phenylalanine (Phe). Due to the presence of Phe intrinsic to the rice grain and Phe in gelatin, a higher signal peak was observed in coated rice grains compared with bare rice grains. In the amide bond region, the amide I and amide III peaks of bare and coated grains had different shapes and intensities. This result was derived from the mechanism involving protein binding inherent to the rice grain, the protein binding between the coating components, and the interaction between the rice grain protein and the coating component.

We specifically investigated the interaction between the rice grains and coating by analyzing the deconvoluted Raman spectra.<sup>29</sup> The deconvoluted C–O–C bending peaks between  $810$  and  $890\text{ cm}^{-1}$  correspond to amylopectin, amylose C1–O–C4, and amylose C1–O–C5 signals. As shown in the zone I spectra in Figure 2C, the coating did not affect the amylopectin C1–O–C6 peak area of rice grains, whereas the amylose C1–O–C4 peak area decreased by 12.73%, and the C1–O–C5 peak area increased by 11.3%. This distinguishable change in amylose bending mode is attributed to hydrogen bonding between starch amylose and Gel/mTG coating. These results demonstrate that the Gel/mTG coating interacts with the amylose of the single helix structure more closely than with the amylopectin of the double helix structure. The bare rice grain exhibited three peaks in the deconvoluted spectra for the secondary structure of proteins: a  $\beta$ -sheet from albumin, an  $\alpha$  helix from prolamin and glutelin, and a random coil from glutelin. Gelatin induces an increase in the  $\alpha$  helix structure and random coil transition of grain protein, resulting in the appearance of overlapping broad peaks in the spectra of rice grains coated with gelatin (Figure 2C, zone II). The mTG mediated the crosslinking of gelatin to gelatin, gelatin to grain protein, and grain protein to grain protein, altering the signal of the protein secondary structure of the coated rice grain. We projected that the Gel/mTG coating would also affect the morphology of rice grains, so we compared the surface morphologies of grain samples using SEM. The low-magnification image revealed a rough and irregular surface of the bare grain, while the high-magnification image revealed a clear granular aggregate shape, indicating the granular morphology of general grains. Due to the Gel/mTG layer, however, the surface of the coated grain exhibited a relatively constant morphology that resembled fish scales in that it was meandering and porous. Upon examination of the enlarged image, it is evident that the exposed granular structure and the coating-covered portion are distinct.

### Crystallinity and structural properties of coated rice grains

A discussion of the crystallinity and  $\Delta H$  of rice grains is necessary to understand the structural stability to increase their cell capacity. As a cellular scaffold, rice grains serve as a support for cells until they differentiate and organize. In other words, the chemical and physical stability of rice grains is a significant factor not only in

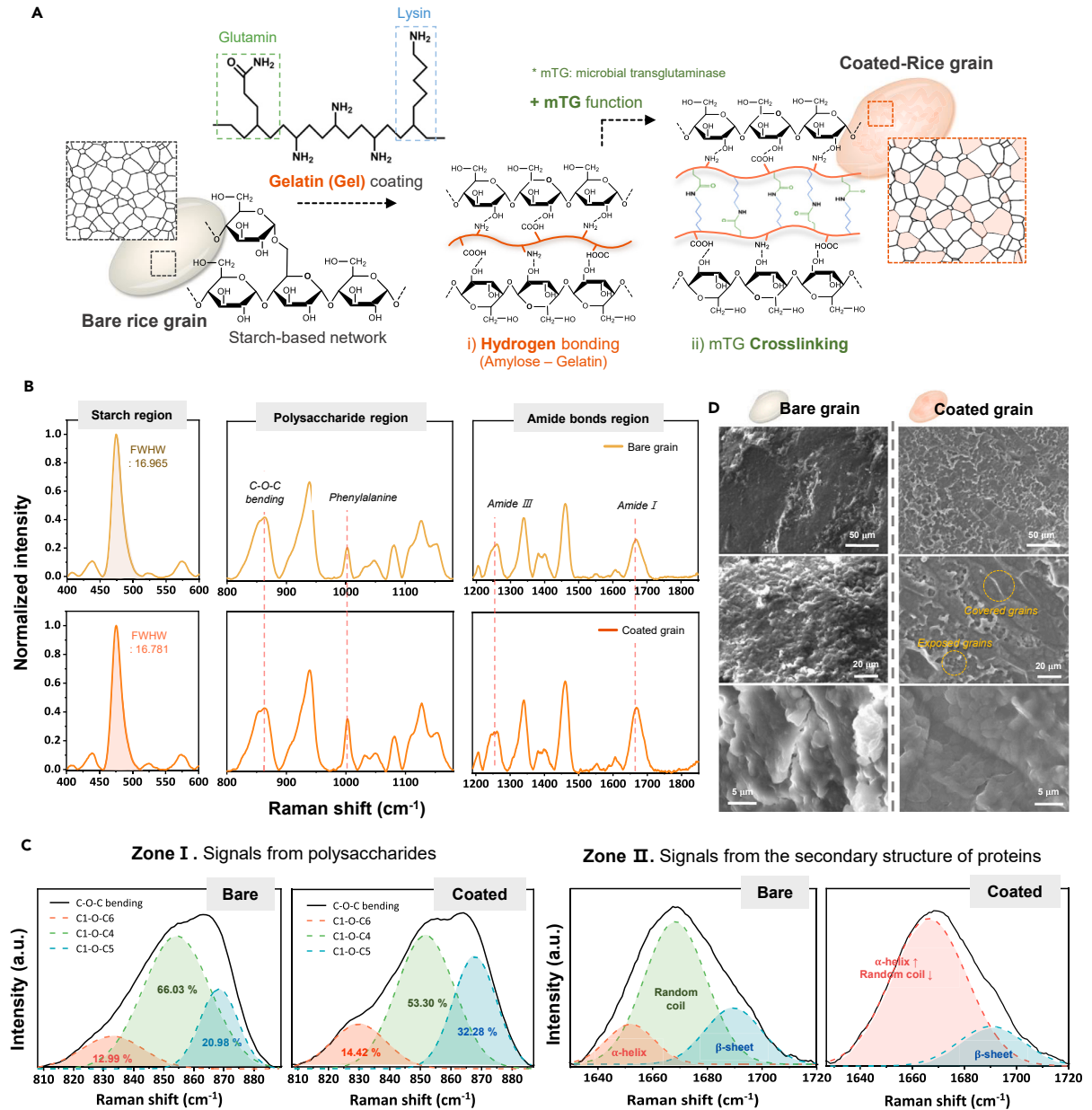


**Figure 2. Preparation of Gel/mTG-coated rice grains**

(A) A schematic of the overall coating principle, in which gelatin is coated on the bare rice grain starch network, followed by the formation of a crosslinked network because of mTG activity.

(B) Raman spectra of bare and coated rice grains to investigate the chemical composition and bond formation of rice grains coated with Gel/mTG. The glucose ring-stretching peak at  $478\text{ cm}^{-1}$  was used as a reference to normalize the overall spectrum of the three regions.

(C) Deconvoluted Raman spectrum C–O–C bending and protein secondary structure signals. The percentage of the total area of each peak is also indicated.

(D) SEM images of bare and coated rice grains for morphological analysis of Gel/mTG coating.



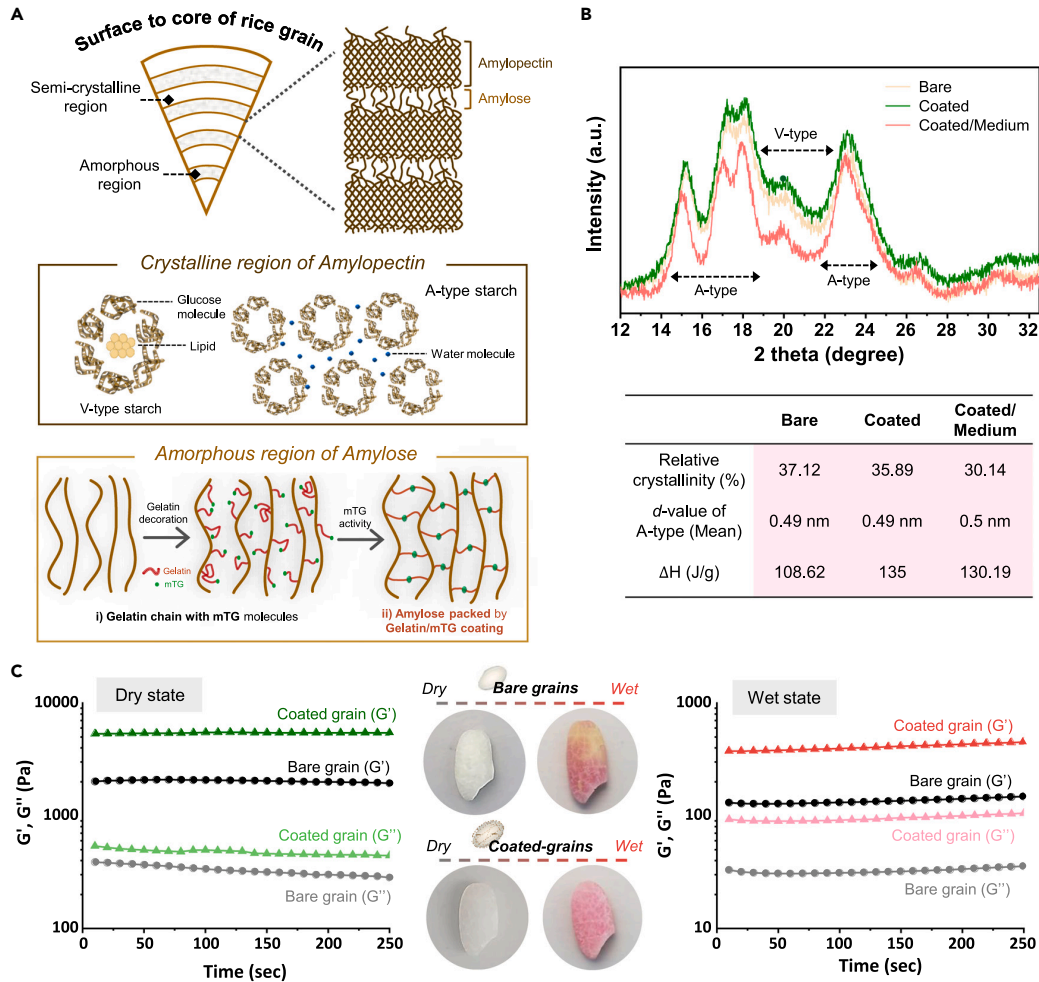


**Figure 3. Effects of coating on structural and physical changes in rice grains**

(A) Schematic of the inner structure of a rice grain, consisting of a starch structure with amylopectin and amylose regions. It depicts the packing of amylose chains using Gel/mTG coating.

(B) Data including the results of XRD spectra and DSC-measured  $\Delta H$ .

(C) Rheometer measurements depicting the storage modulus ( $G'$ ) and loss modulus ( $G''$ ) of bare and coated rice grains in dry and wet states. The modulus under constant strain was measured over time.

cell adhesion but also in cell organization. The growth rings of a rice grain consist of semi-crystalline and amorphous regions. In the semi-crystalline region, amylopectin is responsible for crystallinity, and the double helix of amylopectin is formed by two polyglycosidic chains. Its crystallinity is primarily divided into A-type densely packed glucose helix structures and V-type starch molecules surrounding lipids (Figure 3A). The crystalline region is essential for maintaining grain structure and is closely associated with the rice grains' durability and stability.<sup>30</sup> To produce rice grains with high cell uptake, the coating should not interfere with the grains' crystalline properties. Using X-ray diffraction (XRD) analysis, we investigated the effect of coating on the crystalline properties of rice grains. As shown in the XRD spectra of Figure 3B, distinct A-type and V-type crystallinity were observed in both bare and coated grains, with no significant difference in relative crystallinity between them; that is, 37.12% and 35.89%, respectively; the A-type d value was 0.49 nm (Table S1). In

**Table 1. Summary table for porosimeter data of rice grain samples with different conditions**

	Bare grains	Coated grains	Aged in cell medium	Cell-organized grains
Interparticle porosity (% , $\geq 10 \mu\text{m}$ )	5.3568	8.1129	12.0774	9.3546
Intraparticle porosity (% , $6\text{nm}-10 \mu\text{m}$ )	5.256	3.4524	12.6693	10.9652
Total porosity (%)	10.6128	11.5653	24.7467	20.3198

contrast, the relative crystallinity of coated grain aged for 3 days in cell culture medium decreased significantly to 30.14% because of amylopectin debranching caused by aging and the action of the rice enzyme. The XRD results demonstrated that the Gel/mTG coating has no significant effect on the crystal type and crystallinity of rice grains. Nevertheless, the differential scanning calorimetry (DSC) measurement revealed that the enthalpy change ( $\Delta H$ ) of the bare and coated grains was significantly different: 108.62 J/g and 135 J/g, respectively. Even aged coated grain possessed a higher  $\Delta H$  than bare grain. An increase in  $\Delta H$  indicates an increase in the reassembly or interaction of polymer chains in the rice grain. The improvement of the chemical and physical stability of the rice grain is correlated with a greater interaction between the polymer chains in the rice grain. In addition, these results clarify the Raman spectroscopy findings, demonstrating that the Gel/mTG coating interacts closely with the amylose-containing amorphous region. The gelatin chain activated by mTG forms a hydrogen bond with the amylose single helix, and mTG then forms additional bonds between the amylose chains to form the packed amylose region. The amylose region encapsulated by Gel/mTG coating can enhance the physicochemical stability of rice grains without altering their crystallinity (Figure 3A).

The results of the rheometer measurements depicted the altered physical properties of the rice grains caused by the coating, as shown in Figure 3C. These physical properties not only influence cells from initial attachment to the stage of differentiation but also determine the pasting property of cooked rice. We investigated the dynamic modulus by continuously subjecting dry and wet rice grain samples to a constant shear strain. The storage modulus ( $G'$ ) was higher than the loss modulus ( $G''$ ) for all samples, indicating that the rice grains had elastic properties. For dry samples, the  $G'$  of coated grain was approximately 2.6 times that of bare grain. During the measurement, the  $G''$  of the coated grains tended to decrease slightly after approximately 130 s, whereas the  $G''$  of the bare grains started to decrease gradually after 70 s. Due to the swelling of the amorphous region in the wet samples, both samples exhibited viscoelastic properties, and the dynamic modulus increased with time. Similar to the tendency observed in the dry state, the  $G'$  and  $G''$  of coated grains were significantly greater than those of the bare grains. Furthermore, the chain reassembly of starch by the coating may facilitate the entanglements and interactions of starch molecular chains, thereby forming a strong network structure. Comprehensively, these results show that the coating substantially enhances the physical stability of rice grains, leading to the expectation of improved cell organization in coated rice grains.

The pores and surface area of rice grains are also significant factors in boosting cell capacity. In the porosimeter results presented in Table 1, the change in total porosity due to coating was insignificant, but specific changes in interparticle porosity ( $\geq 10 \mu\text{m}$ ) and intraparticle porosity (6 nm to  $10 \mu\text{m}$ ) were observed. The increase in interparticle porosity caused by the coating is attributed to exposure to moisture and drying during the coating process, while the expected decrease in intraparticle porosity is the result of the nanoblocklet within the coated grain. Considering the size of the cells, this change in porosity creates a favorable environment for



enhancing cell capacity. Incubation of the coated grain in the cell culture medium, however, causes the amorphous region of the grain to expand, resulting in an approximately 2-fold increase in total porosity, thereby facilitating cell incorporation.

#### **Loading and organizing abundant cells in coated rice grains**

The unique and compelling advantages of rice grains as a scaffold for cell organization are that they meet food safety requirements for commercialization and that they provide nutrients to cells. These characteristics enable the creation of a new food ingredient called “rice grains containing animal nutrients.” Considering that cell content significantly impacts the taste and nutritional level of food ingredients, improving the stability of cells to the entire rice grains is a crucial strategy for making high-quality hybrid food. First, we evaluated the nutritional benefits of rice grains to cells. Bovine myoblasts were prepared using the myoblast isolation protocol established in our previous studies.<sup>31</sup> The bovine myoblasts were seeded on the bottom of each well of a Transwell plate, and then rice-containing Transwell inserts were placed in each well. To evaluate the effect of rice grains under fetal bovine serum (FBS)-reduced conditions, proliferation media containing 10% FBS and 5% FBS were used, with the group containing no rice crumbs serving as the control (Figure S1). During the 7-day culture period, the experimental group containing rice crumbs had a 12.82% higher cell proliferation rate than the control group in the 10% FBS group. Compared with the control group, the experimental 5% FBS group had a 16.63% higher proliferation rate, demonstrating the nutritional potential of rice grains for cell proliferation (Figure S1). The higher cell proliferation rate of the rice grain groups was not statistically significant in the FBS 10% group but was significant in the FBS 5% group. In other words, the effect of rice grains on improving cell growth was emphasized under nutritional deficiencies.

Normal rice grains, however, undergo debranching and dissociation due to the activity of rice enzymes when exposed to wet conditions or when stored for an extended period. Since this structural destruction is accelerated by the cell secretome in the cell culture environment, it is challenging to achieve adequate cell organization in normal rice grains. Gel/mTG-coated rice grains, however, can maximize cell capacity due to the coating’s improved structural stability and RGD sequence in addition to their nutritional value. As stated previously, the Gel/mTG coating results in a densely packed amorphous region by inducing additional bonds between amyloses without affecting the crystalline region of the rice grain. Therefore, coated rice grains can serve as a stable scaffold for attaching and connecting numerous cells for organization. Gel/mTG coating has biodegradation properties, providing a suitable environment for the stabilization of cells within rice grains and then slowly being modified and removed.<sup>32</sup> Figure 4 describes the results of the biochemical analysis of the cells in bare and coated rice grains. We first evaluated the proliferation of C2C12, bovine myoblasts, and bovine adMSCs in rice grain samples for 7 days after seeding. The color change of the fresh culture medium replaced daily indicates that the cells are growing in the rice grains (Figure S2). C2C12 and bovine myoblasts demonstrated significantly greater cell proliferation in the coated grain group than in the bare grain group, whereas adMSC proliferation was comparable in both groups. Myoblasts were significantly more affected by substrate stiffness in cell adhesion than adMSCs, resulting in a more pronounced proliferation difference in the myoblast group (Figure 4A). Due to the structural characteristics of the grain, the Cell Counting Kit 8 (CCK-8) assay could not accurately reflect the cell content of the entire grain. Therefore, we performed a DNA quantitative analysis to determine the cell content of the entire grain. A digestion step was performed on rice

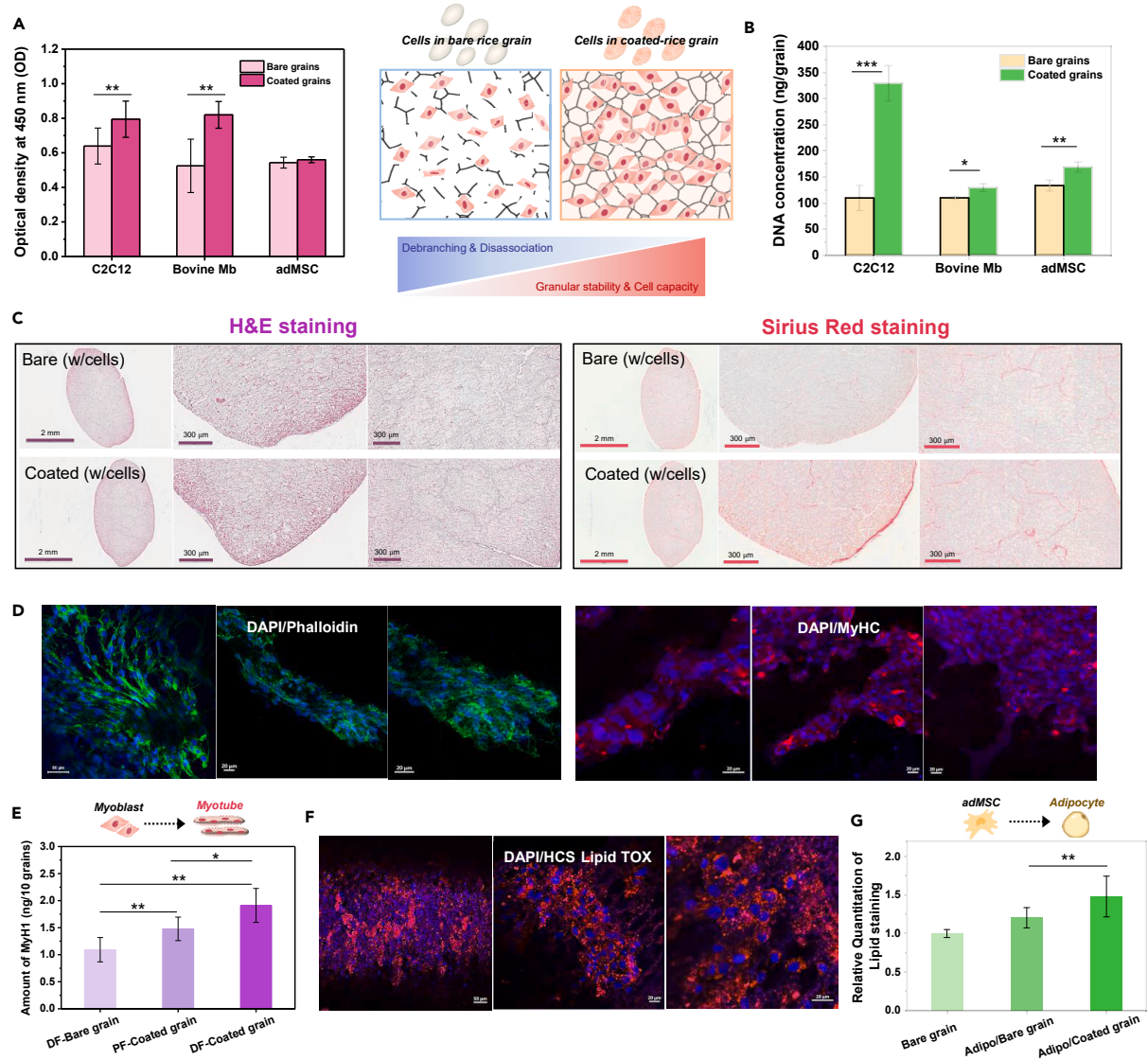


**Figure 4. Biochemical analysis of the cells in rice grains**

These results were obtained from bare and coated rice grains containing cells.

(A) CCK-8 assay data for the proliferation rates of C2C12, bovine myoblasts (bovine Mbs), and bovine adMSCs in the bare and coated grains. The assays were evaluated at  $n = 5$ . The schematic demonstrates the relative density of the cells in the bare grain undergoing chain disassociation and the cells in the coated grain with a stable granular structure during cell proliferation.

(B) Results of quantitative DNA analysis for each rice grain sample in which C2C12, bovine Mbs, and bovine adMSCs proliferated.

(C) Histological analysis of rice grain samples that underwent bovine Mb proliferation and differentiation. H&E staining and Sirius red staining represent cell density and collagen distribution, respectively.

(D) Confocal microscopic images visualized using F-actin (green) stained with Alexa Fluor 488 phalloidin, DAPI-stained nuclei (blue), and MF20-stained MyHC (red). The DAPI/phalloidin staining image shows proliferated bovine Mbs in coated grains. The DAPI/MyHC staining image shows differentiated and organized bovine myotubes within the coated grains.

(E) Quantitative analysis of MyH1 protein to compare the degree of differentiation of bovine Mbs between groups (DF-bare grain, cell differentiated in the bare grain; PF-coated grain, cell proliferated in the coated grain; DF-coated grain, cell-differentiated in the coated grain).

(F) Confocal microscopy images of DAPI/HCS lipid TOX-stained coated grain where the adMSC was differentiated into an adipocyte.

(G) Oil red O staining assay to compare the degree of differentiation into adipocytes.

These quantitative assays were evaluated at  $n = 4$ . A Tukey test of one-way ANOVA was performed for statistical analysis on repeated measurements.

\* $p < 0.05$ , \*\* $p < 0.01$ , \*\*\* $p < 0.001$ .

grain samples to expose the DNA of all cells for the DNA quantitative assay. As shown in [Figure 4B](#), the coated grain group of C2C12 myoblasts contained three times more DNA than the bare grain group. In the coated grain group, the DNA content of bovine myoblast and adMSCs as primary cells was also found to be higher. As depicted in the graph, the effect of coated rice grains was more pronounced in C2C12 myoblast cells, which are more stable than the primary cells. Using bovine myoblasts, we performed histological analysis to visualize the differences in group proliferation. Bovine myoblasts proliferated for 5 days and then differentiated for 4 days. A purple-stained cell region and an unstained granule region were easily distinguished on the hematoxylin and eosin (H&E) images. Some parts of unspecified staining can be explained by the intrinsic staining characteristics of rice grains ([Figure S3](#)). Meanwhile, the highest cell density was observed on the exterior of the rice grain, with a gradual decrease toward the center. As with the results of the cell proliferation assay, the coated grain contained more cells than the bare grain, and this trend was consistent within the rice grain. Gel/mTG solution can coat the entire grain by penetrating the amorphous channels and reaching the interior of the grain. The coated grain exhibited a dense structure and high cell content as a result ([Figure 4C](#)). Sirius red staining is a histochemical method for highlighting collagen networks in connective and muscle tissues. We stained bovine myotubes with Sirius red to visualize their arrangement and organization. As depicted in [Figure 4C](#), the coated grain displayed significantly broader and darker staining than the bare grain, and the distinction was more pronounced than that of the H&E staining.

Immunofluorescence analysis was utilized to observe the precise appearance of proliferating and differentiating cells in the coated rice grains ([Figures 4D](#) and [S4](#)). DAPI/phalloidin images demonstrate that, during the proliferation phase, bovine myoblasts stretched along the granular alignment of the rice grains and formed a network between them. Upon differentiation of bovine myoblasts, DAPI/myosin heavy chain (MyHC) staining images revealed nuclear fusion and cellular aggregation, suggesting differentiation of myoblast to myotube. We quantified the bovine MyH1 protein in samples to confirm the presence of myotubes in rice grains. More MyH1 protein suggests a higher differentiation efficiency of myoblasts into myotubes in rice grains. As depicted in [Figure 4E](#), more MyH1 was detected in the coated grain group that had undergone only the proliferation process (PF-coated grain) than the group differentiated in the bare grain (DF-bare grain). These results indicate that the bare grain does not provide suitable conditions to support myoblast differentiation. As expected, the highest amount of MyH1 was detected in the DF-coated grain, demonstrating its potential as a differentiation scaffold. Because myoblasts are greatly affected by the substrate's stiffness until they are organized, the cell scaffold for myoblast differentiation must have a stable structural scaffold. Due to the packed amylose portion and the coating's protective layer, it was determined that the coated grain exhibited delayed hydrolysis and enzymatic degradation during cell organization. Additionally, liquid chromatography-tandem mass spectrometry (LC-MS/MS) proteomic analysis of DF-coated grains was performed to confirm the presence of several proteins involved in myogenic differentiation. Seven proteins were detected here, including desmin, and these results indicate the formation of myotubes in the coated rice grain samples ([Table S2](#)). Meanwhile, we differentiated adMSCs proliferated from rice grains into adipocytes and observed the emergence of adipocytes in rice grains. The confocal microscopy image revealed the presence of clear adipocytes surrounded by small lipid droplets around the nucleus, indicating that the differentiation of adMSCs into adipocytes in the coated rice grains was successful ([Figure 4F](#)). We utilized an oil red O staining assay to compare the degree of

adipocyte differentiation in each sample.<sup>33</sup> To normalize the lipid staining of the adipocyte group in the bare grain (adipo/bare grain) and the adipocyte group in the coated grain (adipo/coated grain), the lipid staining of the bare grain without cells served as the standard. As anticipated, the adipo/coated grain group exhibited a greater degree of lipid staining than the adipo/bare grain group (Figure 4G). This is attributed to the improved adhesion of adMSCs and the stable structure of the coated rice grains.

### Morphological and texture properties of cell-organized grains

The morphology of cell-organized grains has an important influence on their textural properties<sup>34</sup> as cells undergo proliferation and differentiation and are aligned with the granular rice grains. We confirmed from the porosimeter measurement results (Table 1) that the total porosity of coated rice grains was significantly reduced after the organization of bovine myoblasts, suggesting that the matrix and amorphous channels of the expanded rice grains in the cell medium were blocked by cell organization. In Figure 5, the morphological and mechanical properties of rice grains according to cell organization were investigated. We also analyzed the 3D morphology of bare grains without cells and bovine myoblast-organized coated grains (cell-organized grains) incubated in cell culture by microcomputed tomography (micro-CT) imaging (Figure 5A). To determine the precise effects of cell organization, we subjected bare grains to the cell culture medium for the same amount of time as the samples with organized cells. As depicted in the cross-sectional view, massive cracks progressing in all directions were observed in bare grains, whereas only small cracks were observed in cell-organized grains. Even in the 3D images, the bare grains exhibited a valley-like morphology. Interestingly, in cell-organized grains, relatively regular patterns and smooth morphologies were observed without major defects (Figure 5A). The process of organizing bovine myoblasts on the surface of coated rice grains was detected by scanning electron microscopy (SEM). It was observed that the cells were cultured on the surface of the coated grain with a dense granular structure, and then the cells formed a close cellular network by cell-cell interaction along the granular arrangement of the rice grains. In contrast, when myoblasts proliferated in the bare grain, the cell culture medium and cell secretome eroded the surface, and the cellular network was barely discernible (Figures 5B and S5). We found different shapes and textures between coated and cell-organized grains incubated in the digestion solution. Due to the cell secretome and cell-cell interaction, the coated grain exhibited a brittle, shattered appearance during digestion, whereas the cell-organized grain exhibited a sticky, agglomerated appearance (Figure S6). Given these characteristics, the texture of cell-organized rice must differ from that of normal rice.

Using rheometer measurements, we analyzed the  $G'$  and  $G''$  of steamed cell-organized rice (cell-organized rice) and steamed rice (bare rice) based on changes in shear strain. This analysis showed that the physical properties of the steamed rice changed due to cell organization.  $G'$  reflects the rigid behavior (elastic property) related to the hardness of the rice. Also,  $G''$  indicates the ability of a material to dissipate the energy of deformation, reflecting the viscous properties of rice grains.<sup>35</sup> Cell-organized rice had approximately 4.5 times the initial  $G'$  and 4.2 times the  $G''$  of normal rice, as shown in Figure 5C. Heating denatures actin and myosin, the primary proteins of muscle-related cells and tissues, resulting in a high modulus in cell-organized rice. During denaturation, myosin releases water molecules into the surrounding environment, while actin imparts rigidity and tenacity to rice grains. We evaluated the food texture of steamed rice samples using Texture profile analysis (TPA) analysis. TPA is a popular double compression test for determining the

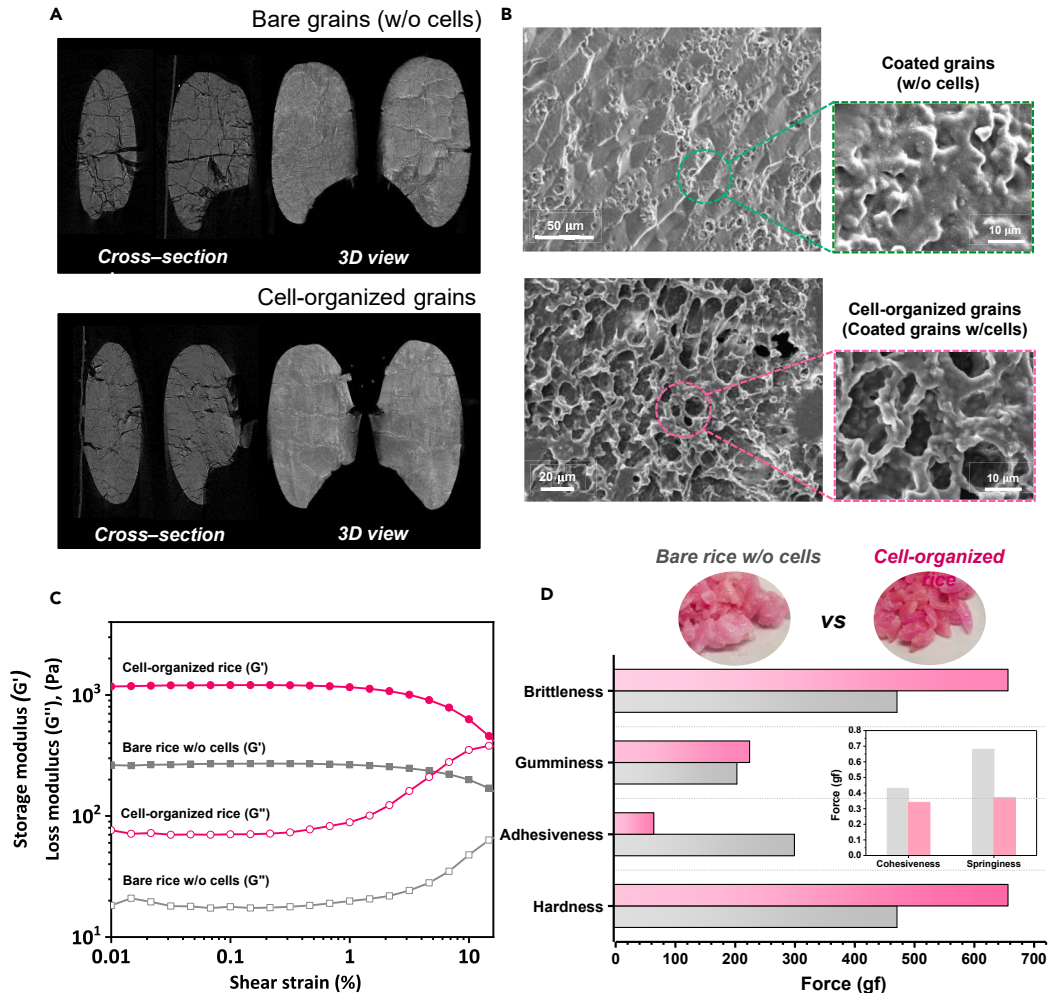


**Figure 5. Analysis of morphological and mechanical properties of rice grains according to cell organization**

Results were obtained from bare grains (without [w/o] cells) and cell-organized grains (Mb-organized coated grains).

(A) Micro-CT observation images of bare grains and cell-organized grains.

(B) SEM images illustrating the morphological distinction between coated grains without cells and cell-organized grains.

(C)  $G'$  and  $G''$  of steamed bare rice and steamed cell-organized rice as measured by the rheometer's strain-sweep mode.

(D) Measuring the textural properties of steamed bare rice and cell-organized rice using a TPA machine.

textural properties of foods. The rice image in Figure 5D illustrates the stark difference in appearance between normal rice and cell-organized rice. Due to the denaturation of actin and myosin present in muscle-related cells and tissues, the brittleness and hardness of cell-organized rice were measured to be greater than those of normal rice. In contrast, adhesiveness and cohesiveness related to viscosity were measured to be notably low in cell-organized rice (Figures 5D and S7). The viscous pasting properties of steamed rice are ascribed to the expansion of the amorphous region and the destruction of the crystalline region.<sup>34</sup> Accordingly, the preceding results suggested that the elongation of starch chains was diminished as coating and cell organization decreased the resistance to amorphous expansion. Combining these results, it is evident that cell organization has a significant impact on the texture of rice grains.



### Nutritional potential of hybrid rice integrated with bovine cells

This study's ultimate objective is to propose a new type of sustainable food ingredient that fuses rice grains and animal cells. Rice grains are predominantly composed of carbohydrates, but they also contain protein, fat, vitamins, and minerals. Therefore, it is possible to ensure a sufficient food supply in the future by integrating animal cells into rice grains to create a new complete meal. We combined bovine myotube-organized rice grain and adipocyte-organized rice grain in equal proportions and dubbed the resulting mixture "hybrid rice." Then, we determined the effect of cell organization on nutritional value by analyzing the nutritional components of bare rice and hybrid rice. The carbohydrate, protein, and fat contents of identically weighted rice samples were determined (Figure 6A). First, hybrid rice contained 0.16 g more carbohydrates than bare rice. This was anticipated because of a delay in carbohydrate decomposition or the binding of carbohydrates to cell components during cell organization in hybrid rice. The crude protein content of hybrid rice was also 310 mg higher than in bare rice. Due to the proliferation and organization of bovine myoblasts, the protein content increased. Given that 1 g of beef brisket contains approximately 186.2 mg of protein, eating 100g of hybrid rice can be described as similar to eating 100 g of bare rice together with 1 g of beef brisket. Although 310 mg per 100 g of rice may seem relatively small, it is worth noting that the cells influence the physical and nutritional properties of the rice grain. Based on understanding these results, more nutritious rice grains could be developed. Hybrid rice contained 10 mg more fat than bare rice. Insufficient differentiation efficiency of adipocytes from adMSCs is responsible for the insignificant difference in fat content compared with other components. Myoblasts are capable of spontaneous and rapid differentiation, whereas the differentiation of adMSCs requires complex conditions. For increased fat content in hybrid rice, it will be necessary in the future to introduce a technology that increases the efficiency of adMSCs to differentiate into adipocytes. We are continuously working to develop a culture medium optimized for differentiation into adipocytes, expecting that the improved adMSC differentiation medium can increase efficient differentiation into adipocytes. Even though bare and hybrid rice grains of equal weight were used in this nutrient analysis, the total number of hybrid grains may be less than that of bare grains because hybrid grains contain cells. However, it is notable that hybrid meat rice contains more carbohydrates, protein, and fat than bare rice.

Since the above nutrient analysis confirmed the increase in protein content due to cell organization, we evaluated the nutritional value of cell-organized rice grains through qualitative analysis of these proteins. Through protein screening and proteomics analysis, we compared proteins expressed in bovine myotube-organized rice (cell-organized rice) and bovine muscle tissue.<sup>15,36</sup> We examined every protein expressed in cell-organized rice grains and bovine muscle tissue. Then, we cataloged proteins whose expression levels in cell-organized rice and bovine tissue differed by less than 1.5-fold (Figure S8). Cell-organized rice expressed a total of 3,048 proteins, of which 565 were identical to those found in bovine tissue. In other words, the cell-organized rice protein was 18.54% genetically identical to the bovine tissue protein (Figure 6B). This suggests that myotubes grown and differentiated from cell-organized rice could exhibit nutritional values comparable with beef. The 565 proteins consistent with bovine tissue proteins were subjected to Gene Ontology (GO) analysis, where the proteins were categorized according to their functions as cellular components (CCs), molecular functions (MFs), and biological processes (BPs).<sup>36</sup> In the GO data sheet, a lower false discovery rate (FDR) and p value indicate a more reliable and enriched GO term. Based on FDR and p value, seven significant terms were chosen and graphed in the CC, MF, and BP categories. As depicted in the



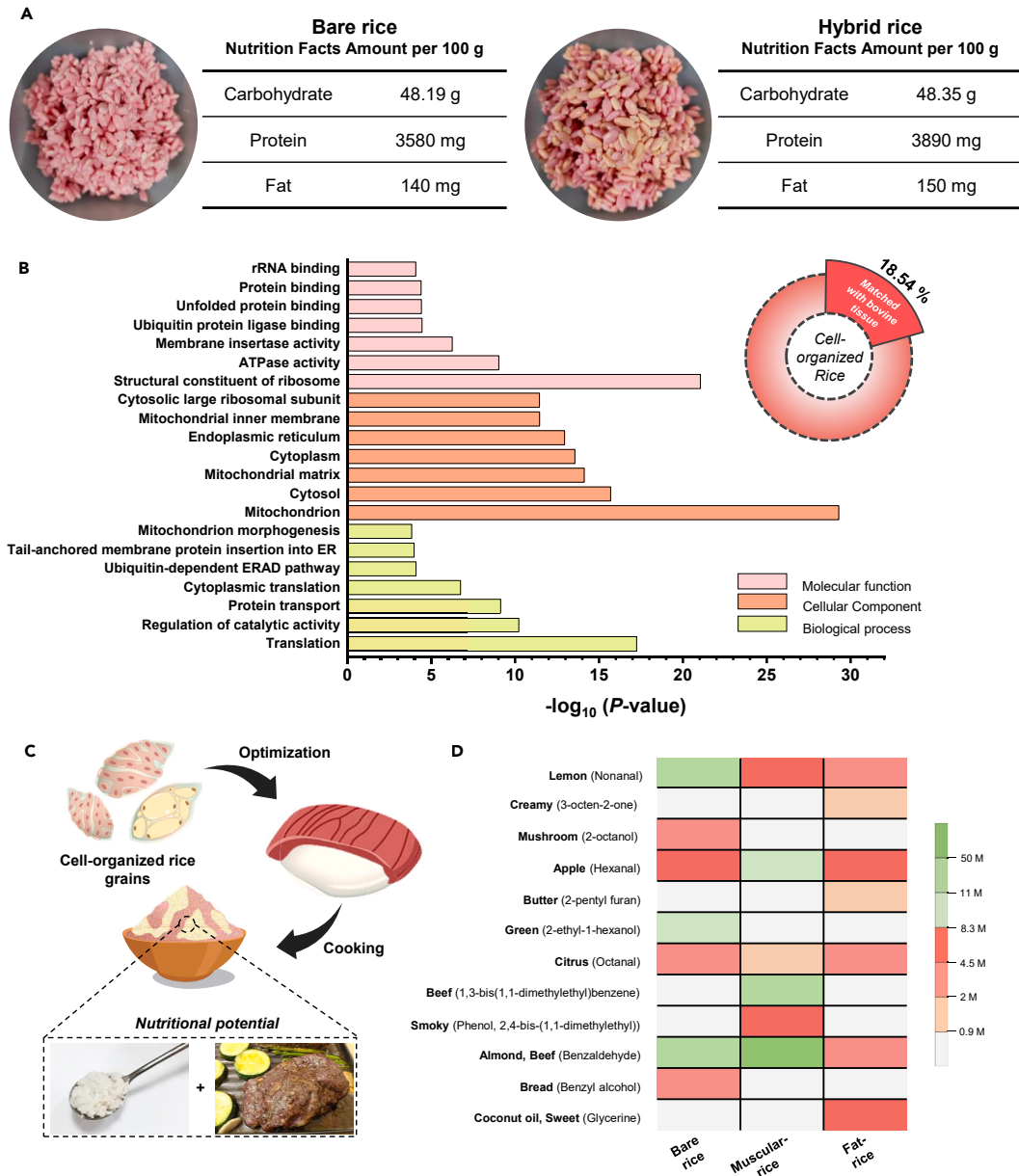


**Figure 6. The nutritional value of hybrid rice**

(A) Results of a food nutrition analysis measuring the protein and fat content of carbohydrate and rice samples.

(B) GO of rice proteins whose expression is consistent with that of bovine tissue. The pie chart depicts the ratio of bovine tissue-matched proteins to total proteins expressed in cell-organized rice. Rice samples that matched bovine tissue contain several significant proteins, as depicted in the bar graph. According to their function, proteins were classified into three subcategories: cellular components (CCs), molecular functions (MFs), and biological processes (BPs).

(C) A diagram of microbeef sushi and microbeef rice that can be produced by optimizing cell-organization rice manufacturing technology as well as their nutritional value.

(D) A heatmap illustrating the flavor intensity of bare rice, muscular rice (myotube-organized rice), and fat rice (adipocyte-organized rice). The color intensity indicates the peak area of the compound detected by GC-MS.

**Table 2. A table to predict the production value of hybrid rice**

Greenhouse gas emissions per 100 g protein (kgCO <sub>2</sub> equiv per 100 g)									
Bovine meat	Rice						Hybrid rice		
49.89 kg	6.27 kg						≤6.27 kg		
Production value per 1 kg of food									
–	Beef (brisket)			Rice			Hybrid rice		
Main nutrients	Carbohydrate	Protein	Fat mineral	Carbohydrate	Protein	Fat mineral	Carbo hydrate	Protein	Fat mineral
	0 g	270 g	200 g	481.9 g	36 g	1.4 g	483.5 g	39 g	1.5 g
Production period	1–3 years			95–250 days			104.75–259.75 days		
Market price	\$14.88			\$2.20			\$2.23		

Shown are the amount of CO<sub>2</sub> gas (kgCO<sub>2</sub>) released to obtain 100 g of protein each from beef, rice, and hybrid rice; the main nutritional components of 1 kg beef, 1 kg rice, and 1 kg hybrid rice, respectively; and their production period and market price (as of May 2023).

bar graph in Figure 6B, components corresponding to CCs are predominantly distributed with high values, which clarifies the effect of organized cells in rice grains. Considering the aforementioned findings, novel fusion foods such as microbeef sushi can be produced by optimizing processes such as co-culturing cells or bonding between rice grains during the preparation of cell-organized rice grains (Figure 6C). This fusion dish could also serve as a complete meal, as it contains both rice and meat.

Using gas chromatography (GC)-MS analysis, we investigated the odor of steamed rice samples (Figure 6D; Table S3). Under identical conditions, bare rice, muscular rice (myotube-organized rice), and fat rice (adipocyte-organized rice) were steamed. After organizing the compounds derived from GC-MS analysis, the flavor corresponding to each compound was identified in the lists of the Flavor Extract Manufacturers Association of the United States (FEMA) and the Joint FAO/World Health Organization (WHO) Expert Committee on Food Additives (JECFA).<sup>37</sup> As shown in Figure 6D, only bare rice contained odor compounds associated with plants and grains, such as mushrooms, green, and bread. Intriguingly, fat-related compounds, such as cream, butter, and coconut oil, were only detected in fat rice, whereas compounds corresponding to beef and almond were abundant in the muscular rice. Accordingly, it was discovered that the flavor of rice grains could vary depending on the type of cell used. We confirmed the value and potential of cell-organized rice samples as food through flavor analysis, one of the most important sensory evaluations of food. Since this research can be applied to grains other than rice, we can develop various types of nutritious grains in the future.

## DISCUSSION

As shown in Table 2, we discussed the production value of these hybrid rice under the assumption that the production process was established. In general, the kgCO<sub>2</sub> produced from 100 g of protein from beef and rice is estimated to be 49.89 kg and 6.27 kg, respectively.<sup>37</sup> The amount of CO<sub>2</sub> from beef is approximately 8 times higher than that from rice. Assuming that a cell line and a mammal-derived component-free culture medium for the production of hybrid rice have been established, the amount of CO<sub>2</sub> released when obtaining 100 g of protein from hybrid rice is expected to be less than 6.27 kg. Meanwhile, it is known that the content of carbohydrates in the nutritional components of beef lean meat (beef brisket) is zero. On the other hand, both regular and hybrid rice contain carbohydrates, proteins, and fats. According to our nutritional content results (Figure 6A), the hybrid rice showed higher carbohydrate, protein, and fat content than regular rice. Although hybrid rice grains still have a lower protein content

than beef, advances in technology that can improve the cell capacity of rice grains will undoubtedly improve the nutritional content of hybrid rice. In terms of the production period, beef usually takes 1–3 years and rice 95–250 days. Considering that we took 9.75 days to organize cells in rice, the production period of hybrid rice is 104.75–259.75 days, and it will be shortened with the development of the production process. Meanwhile, the market price of beef (lean) and rice is \$14.88 and \$2.2 per kg, respectively. Pezzotti et al.<sup>38</sup> estimate that the wholesale cost of cell-cultured meat could be as low as \$63/kg, assuming significant advances in cell culture media and bioreactors. Assuming that the increased amount of nutrients in hybrid rice compared with normal rice shown in Figure 6A is the cell weight in the hybrid rice, 4.8 g of 1 kg of hybrid rice would be the weight of the cells. Based on calculations by Pezzotti et al.,<sup>38</sup> the wholesale price of 4.8 g of cell-cultured meat can be estimated at \$0.03. Therefore, the market price of hybrid rice can be estimated at approximately \$2.23/kg. A scenario based on these predicted figures shows the possibility that the birth of hybrid rice can significantly reduce the problem of CO<sub>2</sub> generation and reach consumers with reasonable nutrition and price.

Meanwhile, all of the rice grains, fish gelatin, and transglutaminase we used in this study can be free from food regulations for commercialization. Furthermore, the fish gelatin coating on the rice grains breaks down slowly during cell differentiation processes and can be completely removed by cooking heat. Fish gelatin is used to include a lot of cells in rice grains, and it decomposes after its role is over. In other words, this rice grain-based hybrid food is made from only edible ingredients, so it does not pose a food safety risk. However, cultured meat researchers need to always consider food safety issues that may arise from cell culture media. To summarize, this rice grain-based meat should be considered a candidate for future food that meets all the criteria for food safety, cell content, nutritional value, and commercial potential. This technology is expected to develop into a system capable of self-producing food in the future and achieve a sustainable food system for the food crisis.

### Conclusions

In this study, a novel food ingredient concept involving the incorporation of animal cells into rice grains coated with edible Gel/mTG is described. Initially, we coated rice grains with Gel/mTG to increase their cell capacity. The coated rice grains were able to organize abundant muscular and fat cells with their RGD sequences and enhanced structural stability. Cell-organized rice grains exhibited distinct morphological and mechanical properties compared with bare rice grains, and these differences influenced the texture of cooked rice significantly. We evaluated the nutritional value and food potential of cell-organized rice by analyzing its nutritional composition, proteomics, and food odor. Hybrid rice contained more protein and fat than bare rice and had a rich flavor. Furthermore, the cell-organized rice (myotube-organized rice) protein was 18.54% genetically identical to the bovine tissue protein. In conclusion, this strategy is a hybrid technology in which food, a scaffold, and cells are mutually beneficial and can be widely applied to other food ingredients by optimizing the interactions between the materials.

### EXPERIMENTAL PROCEDURES

#### Resource availability

##### Lead contact

The lead contact for this manuscript is Dr. Jinkee Hong, who can be contacted at [jinkee.hong@yonsei.ac.kr](mailto:jinkee.hong@yonsei.ac.kr) with any questions regarding the manuscript.

Pdf by:  
<https://www.pro-memoria.info>

#### *Materials availability*

Fish gelatin and mTG were purchased from Geltech and Ajinomoto, respectively. Rice grains harvested in Korea were used in this experiment. High-glucose Dulbecco's modified Eagle's medium (DMEM high glucose), FBS, penicillin-streptomycin-amphotericin (PS), horse serum, and 1× phosphate-buffered saline (PBS [pH 7.4]) were purchased from Thermo Fisher Scientific. Low-glucose DMEM (DMEM low glucose) was purchased from Welgene. Dexamethasone, insulin, ciglitizone, oleic acid, and the lipid (oil red O) staining kit were purchased from Sigma-Aldrich.

#### *Data and code availability*

All data are available in the main text or the [supplemental information](#). The data that support the findings of this study are available from the corresponding author upon reasonable request.

#### **Preparation of Gel/mTG-coated rice grains**

The rice grains utilized in the experiment originated from South Korea. First, a 2 wt % aqueous solution of fish gelatin (from fish skin, molecular weight [MW] 30–50 kDa, Geltech) and mTG (Activa TG-8, Ajinomoto) were prepared. Next, a 1:1 volume ratio of fish gelatin and mTG solution was mixed and stirred at 45°C for 15 min. Before activation, the rice grains were treated with oxygen plasma, after which they were added to the Gel/mTG mixture and held at 40°C for 5 min. The resulting rice grains were then stabilized at room temperature for 10 min before being cooled for 12 h in a refrigerator at 4°C.

#### **Characterization of bare and coated rice grains**

Raman spectroscopy (XploRA Plus, Horiba) was used to study the interaction between the rice grains and Gel/mTG coating. This Raman spectroscopy analysis was performed at an energy intensity of 2.5 mW without photobleaching.<sup>38–40</sup> The morphology of the rice grain samples was examined using field-emission SEM (FE-SEM; JEOS, IT-500HR, USA). Crystallinity analyses of the samples were performed utilizing high-resolution XRD (HR-XRD; Smartlab, Rigaku, Japan). The relative crystallinity was determined by comparing the integrated area of all crystalline peaks with the total integrated area of the crystalline and amorphous region in the deconvoluted XRD spectrum. Next, Bragg's law was used to compute the *d* spacing. DSC (DSC 4000, PerkinElmer, USA) was utilized to measure the  $\Delta H$ . A nitrogen purge gas was utilized to heat up the DSC pan from 20°C to 120°C at a rate of 5°C/min. The  $\Delta H$  was computed using the Pyris software. Rheological characterization of the rice samples was performed at room temperature utilizing a rheometer (MCR 302, Anton Paar, Austria) with 8-mm-diameter parallel plates. The rheological test was conducted in frequency-sweep mode, with the frequencies ranging from 0.1 rad/s to 100 rad/s ( $\gamma = 0.5\%$ ).

#### **Preparation of skeletal muscle and adipose tissues**

The gluteobiceps or semitendinosus muscle and intramuscular or subcutaneous adipose tissues were immediately harvested from male or female Hanwoo cattle aged 29–31 months that were slaughtered at a local abattoir (Kwell, Hongcheon, Korea). adMSCs and myoblasts were subsequently derived from the adipose tissue and skeletal muscle, respectively. All experimental procedures were conducted according to Kangwon National University's Animal Care and Use Guidelines and were approved by the university's institutional animal care and use committee (IACUC) (IACUC approval number KW-220714-1). A specific protocol for the extraction of myoblasts and adMSCs from bovine tissues is outlined in [supplemental experimental procedures S1.1](#) and [S1.2](#).

### Cell culture on rice grains

C2C12, bovine myoblasts, and bovine adMSCs were subcultured on TPP tissue culture dishes at 37°C using a proliferation medium in a 5% CO<sub>2</sub> humidified incubator. The C2C12 and bovine myoblast proliferation medium consisted of DMEM high glucose (Thermo Fisher Scientific) supplemented with 10% FBS (Thermo Fisher Scientific) and 1% PS (Thermo Fisher Scientific). The adMSC proliferation medium consisted of DMEM low glucose (Welgene) supplemented with 10% FBS (Thermo Fisher Scientific) and 1% PS (Thermo Fisher Scientific). All rice grains were sterilized with 70% ethanol and exposed to UV light before being completely dried at room temperature. Each rice grain was placed in a well of 48-well plates. In each well, 10 μL of cell suspension containing  $5 \times 10^3$  cells was added to the grain samples ( $5 \times 10^3$  cells per grain). The rice grains were independently seeded with C2C12 myoblasts (passage 12), bovine myoblasts (passage 2), and bovine adMSCs (passage 2). Cell adhesion was induced in the grains by placing the 48-well plates containing the grains and cell droplets in a cell culture incubator for 2 h. After incubation, each well was filled with 0.5 mL of proliferation medium and incubated for an additional 16 h. Next, the rice grains were transferred to new well plates and allowed to proliferate for 5 or 7 days, replacing the medium daily. After cell proliferation, differentiation was initiated by replacing the differentiation medium of each cell. For myoblast differentiation into myotubes or myofibers, a differentiation medium consisting of DMEM high glucose supplemented with 5% horse serum (Thermo Fisher Scientific) and 1% PS was utilized. DMEM low glucose supplemented with 5% FBS, 1% PS, 4 μM dexamethasone (Sigma-Aldrich), 10 μM insulin (Sigma-Aldrich), 10 μM ciglitazone (Sigma-Aldrich), and 100 μM oleic acid (Sigma-Aldrich) was used for adMSC-to-adipocyte differentiation. For biochemical assays, cells were differentiated for 4 days and then washed in 1× PBS (pH 7.4, Thermo Fisher Scientific). A group of rice grains without cells was also prepared as a control or background group.

### Analysis of cell proliferation and differentiation

The CCK-8 assay (D-Plus CCK Cell Viability Assay Kit, Dongin) and DNA quantification (Quant-iT PicoGreen dsDNA Assay Kit, Invitrogen) were used to evaluate cell proliferation in the rice grain samples. For the CCK-8 assay, washed rice grains were placed in fresh medium after cell proliferation and a 10% (v/v) CCK-8 reagent was added. After a 2-h incubation, 100 μL of the solution from each well was transferred to a 96-well plate, and the absorbance at 450 nm was measured using a microplate reader. Rice grain samples were digested for 4 h with lysate buffer containing Proteinase K (0.5 mg/mL), EDTA solution (5 mM EDTA in 1× PBS), and 0.1% Triton X-100 for DNA quantification. The aqueous working solution was prepared by diluting the double-stranded DNA (dsDNA) reagent 200-fold with 1× TE buffer, following the manufacturer's protocol. The working solution was then added to the supplied standard and digested cell solutions. After 5 min of incubation in a dark room at room temperature, the fluorescence intensity ( $\lambda_{\text{ex}} = 480$  nm and  $\lambda_{\text{em}} = 520$  nm) of the samples was determined using photoluminescence (PL; FP-8300, JASCO). Next, the DNA was quantified by plotting the fluorescence emission intensity versus concentration. Before measuring the absorbance and fluorescence of each group, the normal rice grain group without cells was designated as the blank group in the measurement program. Therefore, the records showed the resulting values with the values of this blank group subtracted.

H&E staining and Sirius red staining were utilized to analyze the histology of cell-containing rice grains. The samples fixed with 10% neutral buffered formalin were formed into blocks and then cut into sliced samples. Next, the samples were

deparaffinized, hydrated, and then stained with the staining solution. The stained slices were scanned digitally using microscope imaging software. H&E histological image analysis of normal rice grains without cells was also performed, using the same method. To detect the cells in the rice grains, confocal laser-scanning microscopy (CLSM; LSM 880, Carl Zeiss) was performed on the DAPI-stained cells (Sigma-Aldrich)/Alexa Fluor 488 phalloidin (Thermo Fisher Scientific), DAPI/MyHC (MF 20, DSHB), and DAPI/HCS Lipid TOX (Thermo Fisher Scientific).

The bovine MYH1 protein of myotubes in the grain samples was quantified using the MYH1 ELISA Kit (MyBioSource). This ELISA was conducted by strictly adhering to the manufacturer's protocol. The differentiation of adMSCs was evaluated using a lipid (oil red O) staining kit (Sigma-Aldrich). For lipid staining, rice grains were fixed with 10% neutral buffered formalin, washed with distilled water, and then soaked for 5 min in 60% isopropanol. A 0.5% (w/v) oil red O solution was prepared using pure isopropanol before being diluted with 6:4 distilled water. The sample dye was dissolved in pure isopropanol, and the intensity was measured at an absorbance of 490 nm.

#### Characterization of bare and cell-organized rice grains

Micro-CT imaging (SkyScan1173; Bruker-CT, Kontich, Belgium) was performed to evaluate the density and structural stability of the bare grain and myotube-organized grains using 2D/3D images. The tube voltage and current for the micro-CT scan were 70 kVp and 114  $\mu$ A, respectively; a 1-mm aluminum filter was also utilized. Next, 800 HR images with a pixel size of 5.36  $\mu$ m and an exposure time of 500 ms (2,240  $\times$  2,240 pixels) were captured. CTvox (v.3.2.0, Bruker-CT) was used to generate 3D images, while Dataviewer (v.1.5.1.2, Bruker-CT) was used to generate cross-sectional images. Finally, FE-SEM (JEOS, IT-500HR) observation of rice grain samples fixed with 10% neutral buffered formalin was performed.

#### Preparation and physical characterization of cooked rice

Rice grain samples sufficiently washed with 1 $\times$  PBS were submerged for 10 min in distilled water to remove cell culture medium and debris. In each experiment, rice grains of identical weight were prepared. The rice grains and water that was twice their weight were placed in a heat-resistant container. The container was placed in a microwave oven for 2 min of cooking, removed, and stored at room temperature for 5 min. This process was repeated once to prepare the steamed rice. Rheological characterization of steamed rice was conducted at room temperature using a rheometer (MCR 302, Anton Paar) equipped with 8-mm-diameter parallel plates. The rheological test was conducted in strain-sweep mode with the strain ranging from 0.01% to 10% ( $\omega = 10$  rad/s). A DSC (DSC 4000, PerkinElmer) analysis was performed on steamed rice to examine the thermal behavior of rice grains based on their cell organization. Using a nitrogen purge gas, the DSC pan was heated from 20°C to 120°C at a rate of 5°C/min.

#### Food potential evaluation of hybrid rice integrated with bovine cells

OATC, a Korean Laboratory Accreditation Scheme (KOLAS)-certified organization, analyzed the nutritional composition of the rice grain samples. For nutritional analysis, we prepared 50 g of bare rice grains and 50 g of cell-organized rice grains. These cell-organized rice grains consisted of an equal number of myotube-organized rice grains and adipocyte-organized rice grains. Samples were digested with sulfuric acid, distilled with a 40% NaOH solution, and titrated with a 0.1 N HCl solution to determine their protein content. The protein content was calculated using the following equation:

$$\text{Protein} \left( \frac{\text{g}}{100\text{g}} \right) = \frac{V_{\text{HCl,used}} \times V_{\text{HCl,blank}} \times M_{\text{HCl}} \times N}{\text{Mass of the specimen (mg)}} \times \text{Nitrogen coefficient} \times 100$$



where  $V_{\text{HCl,used}}$  denotes the volume of HCl used (mL),  $V_{\text{HCl,blank}}$  denotes the volume of HCl in the blank (mL),  $M_{\text{HCl}}$  denotes the molarity of HCl, and  $N$  denotes the atomic weight of nitrogen. Subtracting the mass of the sample's protein, ash, fat, and water from its total mass yielded the carbohydrate content. Using a flame ionization detector, fat content was measured.

TPA was performed at room temperature on steamed rice grain samples using a TXA texture analyzer (Yeonjin, South Korea). In this analysis, a 3-kgf load cell was applied to the samples under ambient humid conditions. We calculated the brittleness, gumminess, adhesiveness, hardness, cohesiveness, and springiness of the samples using the values obtained from the TPA measurement curve following the manufacturer's protocol; the calculation methods are described in [Figure S6](#). Samples of steamed rice were analyzed with GC-MS (Agilent 8890 GC system-Agilent 5677B MSD, Agilent Technologies) for their odor. Rice samples for GC-MS analysis were prepared using headspace-solid phase microextraction (HS-SPME). Volatile and semi-volatile compounds from the specimens were absorbed onto divinylbenzene/carboxen/polydimethylsiloxane fibers. This GC-MS analysis was conducted in splitless mode, with the column oven temperature increased by 4°C/min and remaining at 240°C for 20 min. The peak components separated by GC analysis were identified by comparing the data searched in the spectral library (Agilent Chemstation Integrator) based on the retention time of the standard material and the mass spectrum by GC-MS.

#### **Proteomic analysis process for protein expression study**

In the sampling procedure for proteomic analysis, the cell pellet was lysed and digested using the manufacturer's protocol using an S-Trap Mini Spin Column (Protifi, USA). The samples were homogenized using 5% SDS dissolved in 50 mM TEAB. Next, 100 µg of proteins was heated to 95°C for 5 min, reduced with 5 mM TCEP for 1 h at 60°C, and alkylated with 20 mM iodoacetamide in the dark for 40 min. The alkylated proteins were acidified by adding phosphoric acid and then combined with binding buffer (90% methanol, 100 mM TEAB [pH 7.1]). After mixing the protein solution thoroughly, it was filtered and centrifuged at 4,000 × *g* for 30 s. Then the samples were washed thrice with a solution of 90:10 methanol:50 mM TEAB and digested with trypsin gold (Promega) at 37°C overnight at a protein-to-enzyme ratio of 10:1 (w/w). The obtained peptides were successively eluted in three elution buffers containing 50 mM TEAB, 0.2% formic acid, and 50% acetonitrile/0.2% formic acid in water. Next, 100 µg of each peptide sample was labeled with 16-plex TMT reagent (Thermo Fisher Scientific, Rockford, IL, USA) according to the manufacturer's protocol. After combining all labeled peptides, high-pH reverse-phase LC (RPLC) fractionation was performed using a NexeraXR HPLC system (Shimadzu). Briefly, the desalted peptide mixture was injected into a column (4.6 × 250 mm, 5 µm) and fractionated into 20 components using high-pH buffer A (10 mM ammonium formate in water [pH 10]) and buffer B (10 mM ammonium formate in 90% acetonitrile [pH 10]). The separated peptides were collected non-contiguously, dried in a high-speed vacuum, and stored at -80°C. The peptides were analyzed using an LC-MS/MS system comprised of an UltiMate 3000 RSLCnano system (Thermo Fisher Scientific) and an Orbitrap Eclipse Tribrid mass spectrometer (Thermo Fisher Scientific) with a nano-electrospray source (EASY-Spray Sources, Thermo Fisher Scientific). The expression of genes associated with the detected proteins was investigated in DAVID Bioinformatics Resources.<sup>41</sup>

#### **SUPPLEMENTAL INFORMATION**

Supplemental information can be found online at <https://doi.org/10.1016/j.matt.2024.01.015>.

## ACKNOWLEDGMENTS

This research was supported by the Bio & Medical Technology Development Program of the National Research Foundation (NRF), funded by the Ministry of Science & ICT (2019M3A9H110378622); the Korea Drug Development Fund, funded by Ministry of Science and ICT, Ministry of Trade, Industry, and Energy and Ministry of Health and Welfare (HN21C141000023, Republic of Korea); and the National Research Foundation of Korea (NRF) grant funded by the Korea government (MSIT) (2021R1A4A3030268).

## AUTHOR CONTRIBUTIONS

Conceptualization, S.P. and J.H.; methodology, S.P., M.L., H.L., J.M.L., and S.T.L.; investigation, S.P., B.C., and W.-G.K.; visualization, G.B., H.H., K.H.Y., and D.H.; supervision, S.L. and J.H.; writing – original draft, S.P. and S.J.; writing – review & editing, S.P., J.H., and S.L.

## DECLARATION OF INTERESTS

The authors declare no competing interests.

Received: July 26, 2023

Revised: November 20, 2023

Accepted: January 11, 2024

Published: February 14, 2024

**Pdf by:**  
<https://www.pro-memoria.info>

## REFERENCES

- Bodirsky, B.L., Chen, D.M.-C., Weindl, I., Soergel, B., Beier, F., Molina Bacca, E.J., Gaupp, F., Popp, A., and Lotze-Campen, H. (2022). Integrating degrowth and efficiency perspectives enables an emission-neutral food system by 2100. *Nat. Food* 3, 341–348.
- Duarte, C.M., Bruhn, A., and Krause-Jensen, D. (2021). A seaweed aquaculture imperative to meet global sustainability targets. *Nat. Sustain.* 5, 185–193.
- Stephens, E.C., Martin, G., Van Wijk, M., Timsina, J., and Snow, V. (2020). Impacts of COVID-19 on agricultural and food systems worldwide and on progress to the sustainable development goals. *Agric. Syst.* 183, 102873.
- Fan, S., Teng, P., Chew, P., Smith, G., and Copeland, L. (2021). Food system resilience and COVID-19—Lessons from the Asian experience. *Glob. Food Sec.* 28, 100501.
- Lindgren, E., Harris, F., Dangour, A.D., Gasparatos, A., Hiramatsu, M., Javadi, F., Loken, B., Murakami, T., Scheelbeek, P., and Haines, A. (2018). Sustainable food systems—a health perspective. *Sustain. Times* 13, 1505–1517.
- Schulte, L.A., Dale, B.E., Bozzetto, S., Liebman, M., Souza, G.M., Haddad, N., Richard, T.L., Basso, B., Brown, R.C., Hilbert, J.A., and Arbuckle, J.G. (2021). Meeting global challenges with regenerative agriculture producing food and energy. *Nat. Sustain.* 5, 384–388.
- McGreevy, S.R., Rupprecht, C.D.D., Niles, D., Wiek, A., Carolan, M., Kallis, G., Kantamaturapoj, K., Mangnus, A., Jehlička, P., Taherzadeh, O., et al. (2022). Sustainable agrifood systems for a post-growth world. *Nat. Sustain.* 5, 1011–1017.
- Kołodziejczak, K., Onopiuk, A., Szpicer, A., and Poltorak, A. (2021). Meat analogues in the perspective of recent scientific research: A review. *Foods* 11, 105.
- Marvin, H.J., Bouzembrak, Y., Van der Fels-Klerx, H., Kempenaar, C., Veerkamp, R., Chauhan, A., Stroosnijder, S., Top, J., Simsek-Senel, G., Vrolijk, H., et al. (2022). Digitalisation and artificial intelligence for sustainable food systems. *Trends Food Sci. Technol.* 120, 344–348.
- Noort, M.W.J., Renzetti, S., Linderhof, V., du Rand, G.E., Marx-Pienaar, N.J.M.M., de Kock, H.L., Magano, N., and Taylor, J.R.N. (2022). Towards sustainable shifts to healthy diets and food security in sub-Saharan Africa with climate-resilient crops in bread-type products: A food system analysis. *Foods* 11, 135.
- van Dijk, B., Jouppila, K., Sandell, M., and Knaapila, A. (2023). No meat, lab meat, or half meat? Dutch and Finnish consumers' attitudes toward meat substitutes, cultured meat, and hybrid meat products. *Food Qual.* 108, 104886.
- Grasso, S., and Jaworska, S. (2020). Part meat and part plant: Are hybrid meat products fad or future? *Foods* 9, 1888.
- Kim, T.-K., Yong, H.I., Cha, J.Y., Park, S.-Y., Jung, S., and Choi, Y.-S. (2022). Drying-induced restructured jerky analog developed using a combination of edible insect protein and textured vegetable protein. *Food Chem.* 373, 131519.
- Young, J.F., and Skrivergaard, S. (2020). Cultured meat on a plant-based frame. *Nat. Food* 1, 195.
- Ben-Arye, T., Shandalov, Y., Ben-Shaul, S., Landau, S., Zagury, Y., Ianovici, I., Lavon, N., and Levenberg, S. (2020). Textured soy protein scaffolds enable the generation of three-dimensional bovine skeletal muscle tissue for cell-based meat. *Nat. Food* 1, 210–220.
- Andreassen, R.C., Rønning, S.B., Solberg, N.T., Grønlien, K.G., Kristoffersen, K.A., Høst, V., Kolset, S.O., and Pedersen, M.E. (2022). Production of food-grade microcarriers based on by-products from the food industry to facilitate the expansion of bovine skeletal muscle satellite cells for cultured meat production. *Biomaterials* 286, 121602.
- Su, L., Jing, L., Zeng, X., Chen, T., Liu, H., Kong, Y., Wang, X., Yang, X., Fu, C., Sun, J., and Huang, D. (2023). 3D-Printed prolamin scaffolds for cell-based meat culture. *Adv. Mater.* 35, 2207397.
- Chen, Y., Li, L., Chen, L., Shao, W., Chen, X., Fan, X., Liu, Y., Ding, S., Xu, X., Zhou, G., and Feng, X. (2023). Gellan gum-gelatin scaffolds with Ca<sup>2+</sup> crosslinking for constructing a structured cell cultured meat model. *Biomaterials* 299, 122176.
- Mohidem, N.A., Hashim, N., Shamsudin, R., and Che Man, H. (2022). Rice for food security: Revisiting its production, diversity, rice milling process and nutrient content. *Agriculture* 12, 741.
- Gul, K., Yousuf, B., Singh, A., Singh, P., and Wani, A.A. (2015). Rice bran: Nutritional values and its emerging potential for development of

- functional food—A review. *Bioact. Carbohydr. Diet. Fibre* 6, 24–30.
21. Bhullar, N.K., and Gruissem, W. (2013). Nutritional enhancement of rice for human health: the contribution of biotechnology. *Biotechnol. Adv.* 31, 50–57.
  22. Hwang, S.Y., Kang, Y.J., Sung, B., Jang, J.Y., Hwang, N.L., Oh, H.J., Ahn, Y.R., Kim, H.J., Shin, J.H., Yoo, M.a., et al. (2018). Folic acid is necessary for proliferation and differentiation of C2C12 myoblasts. *J. Cell. Physiol.* 233, 736–747.
  23. Zeng, H. (2009). Selenium as an essential micronutrient: roles in cell cycle and apoptosis. *Molecules* 14, 1263–1278.
  24. Wu, P., Li, C., Bai, Y., Yu, S., and Zhang, X. (2019). A starch molecular basis for aging-induced changes in pasting and textural properties of waxy rice. *Food Chem.* 284, 270–278.
  25. Patindol, J.A., Siebenmorgen, T.J., and Wang, Y.J. (2015). Impact of environmental factors on rice starch structure: A review. *Starch-Stärke* 67, 42–54.
  26. Bao, J. (2019). In *Rice starch*, Rice, ed. (Elsevier), pp. 55–108.
  27. Zhu, Y., and Tramper, J. (2008). Novel applications for microbial transglutaminase beyond food processing. *Trends Biotechnol.* 26, 559–565.
  28. McDermott, M.K., Chen, T., Williams, C.M., Markley, K.M., and Payne, G.F. (2004). Mechanical properties of biomimetic tissue adhesive based on the microbial transglutaminase-catalyzed crosslinking of gelatin. *Biomacromolecules* 5, 1270–1279.
  29. Pezzotti, G., Zhu, W., Chikaguchi, H., Marin, E., Boschetto, F., Masumura, T., Sato, Y.-I., and Nakazaki, T. (2021). Raman molecular fingerprints of rice nutritional quality and the concept of Raman barcode. *Front. Nutr.* 8, 663569.
  30. Wang, H., Wang, Y., Wang, R., Liu, X., Zhang, Y., Zhang, H., and Chi, C. (2022). Impact of long-term storage on multi-scale structures and physicochemical properties of starch isolated from rice grains. *Food Hydrocoll.* 124, 107255.
  31. Park, S., Lee, H., Jung, S., Choi, B., Lee, M., Jung, S.Y., Lee, S.T., Lee, S., and Hong, J. (2023). Cost-Effective Culture Medium for Cell-Based Future Foods. *ACS Sustain. Chem. Eng.* 11, 13868–13876.
  32. Gupta, D., Santoso, J.W., and McCain, M.L. (2021). Characterization of gelatin hydrogels cross-linked with microbial transglutaminase as engineered skeletal muscle substrates. *Bioengineering* 8, 6.
  33. Koopman, R., Schaart, G., and Hesselink, M.K. (2001). Optimisation of oil red O staining permits combination with immunofluorescence and automated quantification of lipids. *Histochem. Cell Biol.* 116, 63–68.
  34. Yu, L., Witt, T., Rincon Bonilla, M., Turner, M., Fitzgerald, M., and Stokes, J. (2019). New insights into cooked rice quality by measuring modulus, adhesion and cohesion at the level of an individual rice grain. *J. Food Eng.* 240, 21–28.
  35. Zhu, L., Wu, G., Cheng, L., Zhang, H., Wang, L., Qian, H., and Qi, X. (2019). Effect of soaking and cooking on structure formation of cooked rice through thermal properties, dynamic viscoelasticity, and enzyme activity. *Food Chem.* 289, 616–624.
  36. Ribeiro, S., Ribeiro, C., Martins, V.M., Honoré, B., Neves-Petersen, M.T., Gomes, A.C., and Lanceros-Mendez, S. (2022). Understanding Myoblast Differentiation Pathways When Cultured on Electroactive Scaffolds through Proteomic Analysis. *ACS Appl. Mater. Inter.* 14, 26180–26193.
  37. Lee, M., Park, S., Choi, B., Kim, J., Choi, W., Jeong, I., Han, D., Koh, W.-G., and Hong, J. (2022). Tailoring a Gelatin/Agar Matrix for the Synergistic Effect with Cells to Produce High-Quality Cultured Meat. *ACS Appl. Mater. Inter.* 14, 38235–38245.
  38. Pezzotti, G., Zhu, W., Hashimoto, Y., Marin, E., Masumura, T., Sato, Y.-I., and Nakazaki, T. (2021). Raman Fingerprints of Rice Nutritional Quality: A Comparison between Japanese Koshihikari and Internationally Renowned Cultivars. *Foods* 10, 2936.
  39. Pezzotti, G., Zhu, W., Chikaguchi, H., Marin, E., Boschetto, F., Masumura, T., Sato, Y.-I., and Nakazaki, T. (2021). Raman molecular fingerprints of rice nutritional quality and the concept of Raman barcode. *Front. Nutr.* 8, 663569.
  40. Matteini, P., Cottat, M., Tavanti, F., Panfilova, E., Scuderi, M., Nicotra, G., Menziani, M.C., Khlbtsov, N., de Angelis, M., and Pini, R. (2017). Site-selective surface-enhanced Raman detection of proteins. *ACS Nano* 11, 918–926.
  41. Choi, B., Park, S., Lee, M., Jung, S., Lee, H., Bang, G., Kim, J., Hwang, H., Yoo, K.H., Han, D., et al. (2023). High protein-containing new food by cell powder meat. *NPJ Sci. Food* 7, 13.

**Matter, Volume 7**

## **Supplemental information**

**Rice grains integrated with animal cells:**

**A shortcut to a sustainable food system**

**Sohyeon Park, Milae Lee, Sungwon Jung, Hyun Lee, Bumgyu Choi, Moonhyun Choi, Jeong Min Lee, Ki Hyun Yoo, Dongoh Han, Seung Tae Lee, Won-Gun Koh, Geul Bang, Heeyoun Hwang, Sangmin Lee, and Jinkee Hong**

Pdf by:  
<https://www.pro-memoria.info>

Supplemental information

## **Rice grains integrated with animal cells: A Shortcut to a Sustainable Food System**

**<sup>a</sup>Sohyeon Park, <sup>a</sup>Milae Lee <sup>a</sup>Sungwon Jung, <sup>b</sup>Hyun Lee, <sup>a</sup>Bumgyu Choi, <sup>a</sup>Moonhyun Choi  
<sup>b</sup>Jeong Min Lee, <sup>c</sup>Ki Hyun Yoo, <sup>c</sup>Dongoh Han, <sup>b</sup>Seung Tae Lee, <sup>a</sup>Won-Gun Koh, <sup>d</sup>Geul  
Bang, <sup>d</sup>Heeyoun Hwang, <sup>e</sup>Sangmin Lee\*\*, <sup>a</sup>Jinkee Hong\*<sup>§</sup>**

PDF by:  
<https://www.pro-memoria.info>

<sup>a</sup> Department of Chemical & Biomolecular Engineering, College of Engineering, Yonsei University, 50 Yonsei-ro, Seodaemun-gu, Seoul 03722, Republic of Korea

<sup>b</sup> Department of Animal Life Science, Kangwon National University, 1 Kangwondaehak-gil, Chuncheon-si, Gangwon-do 24341, Republic of Korea

<sup>c</sup> Simple Planet, Inc., 34, Sangwon 12-gil, Seongdong-gu, Seoul 04790, Republic of Korea

<sup>d</sup> Research Center for Bioconvergence Analysis, Korea Basic Science Institute, 162 Yeongudanji-ro, Cheongju-si, Chungbuk 28119, Republic of Korea

<sup>e</sup> School of Mechanical Engineering, Chung-Ang University, 84 Heukseuk-ro, Dongjack gu, Seoul 06974, Republic of Korea

\*The first corresponding author's email address: [jinkee.hong@yonsei.ac.kr](mailto:jinkee.hong@yonsei.ac.kr)

\*\*The second corresponding author's email address: [slee98@cau.ac.kr](mailto:slee98@cau.ac.kr)

<sup>§</sup>Lead Contact's email address: [jinkee.hong@yonsei.ac.kr](mailto:jinkee.hong@yonsei.ac.kr)

## **1. Supplemental Experimental Procedures**

### **S1.1. Retrieval of myoblasts from bovine skeletal muscle tissues**

The harvested muscle tissues were washed sequentially in 70 % ethanol (Samchun Chemical, Seoul, Korea) and 2 % (v/v) antibiotic-antimycotic solution (Welgene, Daegu, Korea) diluted in Dulbecco's phosphate-buffered saline (DPBS; Welgene). After cutting the muscle tissues into small pieces, the pieces were digested at 37°C for 30 min with 0.2 % (w/v) collagenase type II (Worthington Biochemical Corporation, Lakewood, NJ, USA) dissolved in HG-DMEM. The fragmented muscle tissues were incubated for 5 min at 37 °C in high-glucose Dulbecco's Modified Eagle Medium (HG-DMEM; Welgene) containing 1 % (w/v) pronase (Calbiochem, Darmstadt, Germany). The fully digested skeletal muscle tissues were then resuspended in HG-DMEM supplemented with 2 % (v/v) heat-inactivated fetal bovine serum (FBS; Welgene) for dissociation enzyme inactivation. After centrifuging at  $1500 \times g$  for 4 min, the pellets were resuspended in RBC lysis buffer (Sigma-Aldrich, St. Louis, MO, USA) for 10 min at room temperature to remove red blood cells (RBCs). The RBC-free primary cells were filtered using a 100- $\mu\text{m}$  cell strainer (SPL, Pocheon, Korea), followed by filtration through a 70- $\mu\text{m}$  cell strainer (SPL). After 4 min of centrifugation at  $1500 \times g$ , the muscle-derived primary cells were resuspended in HG-DMEM supplemented with 10 % (v/v) FBS, 5 ng/ml basic fibroblast growth factor (bFGF; Peprotech, Rocky Hill, NJ, USA), and 1 % (v/v) antibiotic-antimycotic (herein referred to as myoblast proliferation medium). To isolate myoblasts from muscle-derived primary cells, muscle-derived primary cells ( $5 \times 10^5$ ) were seeded onto a 35-mm culture dish (SPL) and cultured in a myoblast proliferation medium. Non-adherent cells were removed from the culture dishes after 24 hours, and the remaining adherent cells were cultured at 37 °C in a humidified atmosphere of 5% CO<sub>2</sub> in the air, with medium exchanges occurring every two days. When cell confluency reached 50-60 %, adherent cells were collected by



incubating them with 0.05 % trypsin-EDTA (Welgene), and the collected myoblasts were used in the subsequent experiments.

### **S1.2. Retrieval of MSCs from bovine adipose tissues**

The harvested adipose tissues were successively washed once in 70 % ethanol and twice in a diluted 2 % (v/v) antibiotic-antimycotic solution in DPBS. The clean adipose tissues were then cut into small pieces using surgical scissors, and the small pieces were dispersed at 37 °C for 30 min using 0.75 % (w/v) collagenase type II dissolved in 0.25 % trypsin-EDTA. During the dispersion procedure, small tubes containing digested adipose tissues were vigorously shaken up and down at 5 min intervals for 30 min at 37 °C. For dissociation enzyme inactivation, 10 % (v/v) FBS was added to Dulbecco's Modified Eagle Medium (LG-DMEM; Welgene). Following filtration with a 100- $\mu$ m cell strainer, the pellets resulting from centrifugation at 415  $\times$  g for 5 min were resuspended in RBC lysis buffer for 10 min at room temperature to eliminate RBCs. The RBC-free primary cells were then separated by centrifugation at 415  $\times$  g for 5 min and resuspended in LG-DMEM supplemented with 10 % (v/v) FBS and 1 % (v/v) antibiotic-antimycotic solution (herein referred to as ADMSC proliferation medium). To isolate MSCs from adipose tissue-derived primary cells, adipose-derived primary cells ( $1 \times 10^4$ ) were seeded onto a 35-mm culture dish and cultured for 6-8 days in ADMSC proliferation medium at 37°C in a humidified atmosphere of 5 % CO<sub>2</sub> and air. Then, non-adherent cells to the culture dishes were discarded by exchanging ADMSC proliferation medium at two-day intervals, and colony-forming units-fibroblast (CFU-F) formed on the culture dishes were harvested with 0.2 5% trypsin-EDTA, and the harvested ADMSCs were utilized in the subsequent experiments.

## 2. Figure section

**Cells:** Bovine myoblast

**Period of proliferation:** 7 days

**Medium change:** Once in 3 days

**Control groups:** FBS 10% GM and FBS 5% GM

**Experimental groups:** Rice grain/FBS 10% and Rice grain/FBS 5%

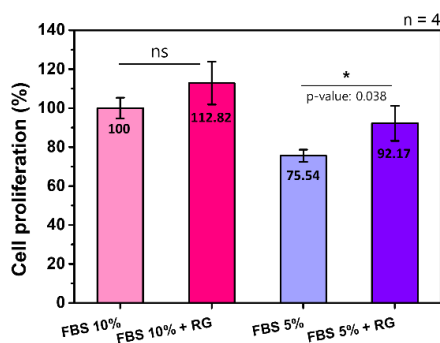


**Figure S1.** CCK-assay results using transwell inserts containing rice grain crumbs to evaluate the nutritional effect of rice grains on cell proliferation (N = 4). The graph was expressed as a percentage of normalized cell proliferation relative to a 10% FBS medium group. A Turkey test of One-way ANOVA was performed for statistical analysis on repeated measurements. \*P-value <0.05, \*\*P-value <0.01, \*\*\*P-value <0.001.

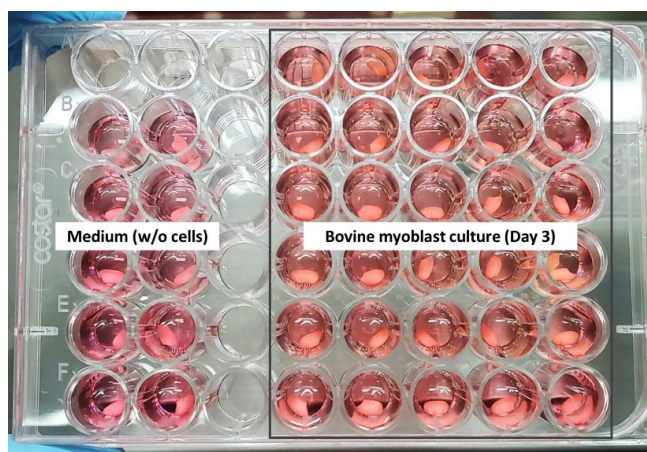


**Figure S2.** Cultivation of bovine myoblast in rice grains (Day 3). A cell-free medium group was also included to show the change in medium color according to cell proliferation. We replaced all groups' mediums with fresh mediums 24 hours before this photo was taken.

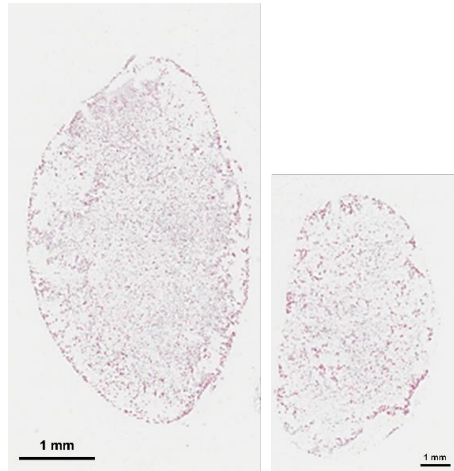


**Figure S3.** H&E staining image for histological analysis of normal rice grains without cells. Stained grain flakes were shown as small images.

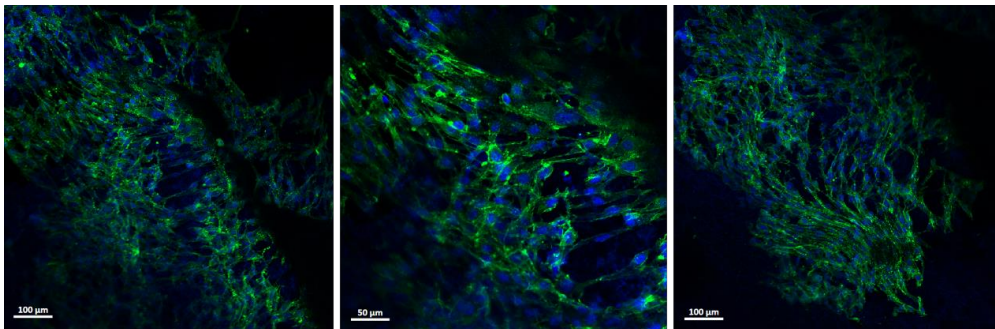


**Figure S4.** Confocal microscopic images showing proliferated bovine myoblasts in coated grains. The images were visualized using F-actin (green) stained with Alexa Fluor® 488 phalloidin, DAPI-stained nuclei (blue).

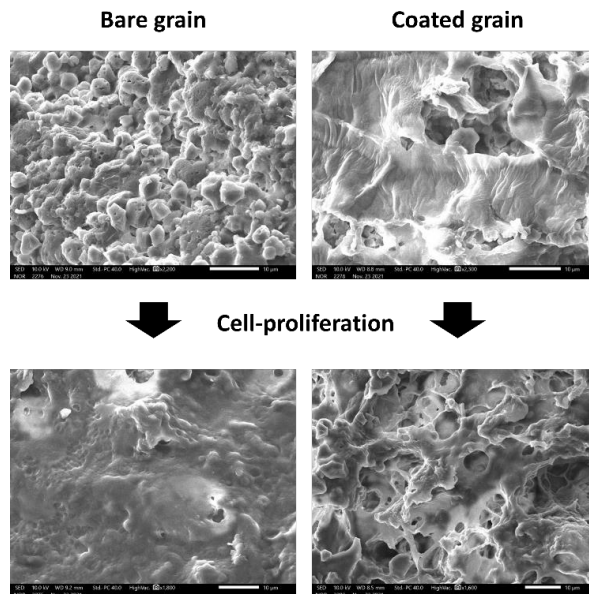


**Figure S5.** SEM images illustrate the morphological difference between uncoated and coated grain before and after cell proliferation.

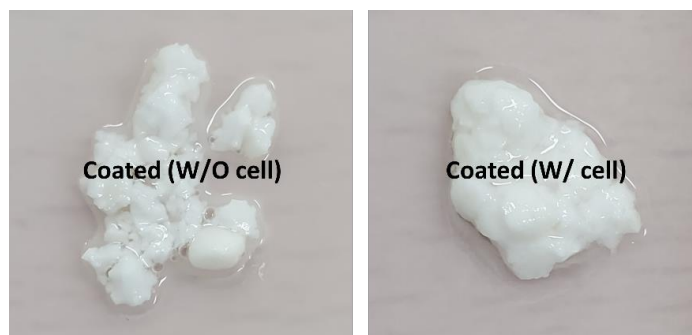


**Figure S6.** Images comparing the appearance of coated grain and cell-organized grain (Coated W/cell) following digestion.



	Hardness	Adhesiveness	Cohesiveness	Gumminess	Brittleness	Springiness
Bare rice	470.72	299.17	0.43	202.82	470.66	0.68
Cell-organized rice	656.48	63.90	0.34	224.17	656.42	0.37

**Figure S7.** Measurement graphs of texture profile analysis for uncoated rice and cell-organized rice, as well as each value for six textures derived from the graphs.

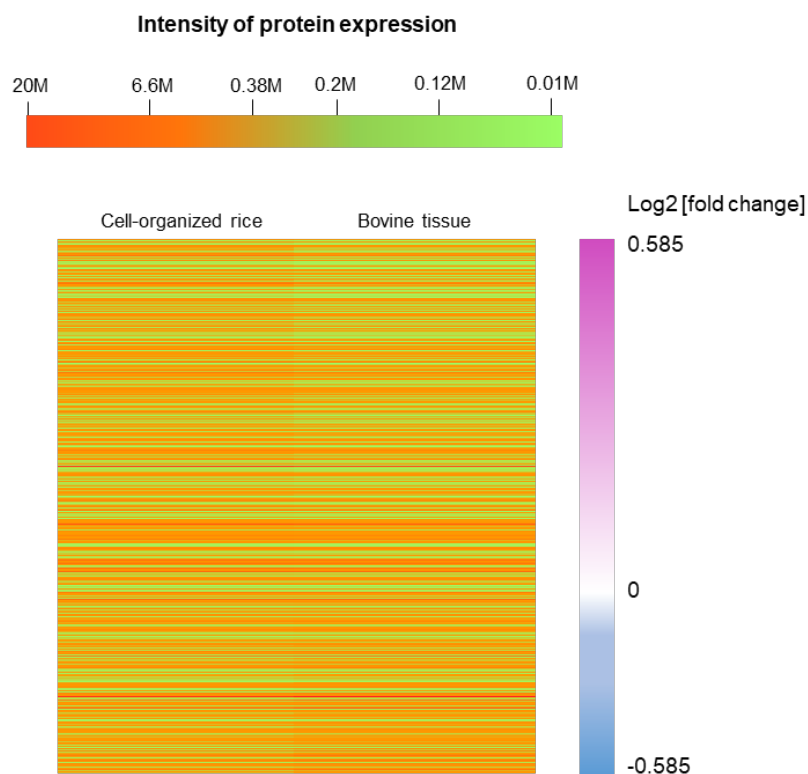


**Figure S8.** A heat map of proteins expressed in cell-organized rice and bovine tissue with an

intensity difference of less than 1.5-fold. The band of color on the right represents the log<sub>2</sub> value (cell-organized rice/bovine tissue). The upward movement of purple indicates 1.5 times greater expression in rice, whereas the downward movement of blue indicates greater expression in tissue.

### 3. Table section

	<i>d</i> -spacing (nm) calculated by XRD data				
	<b>A-type 1</b>	<b>A-type 2</b>	<b>A-type 3</b>	<b>V-type</b>	<b>A-type 4</b>
<b>Bare rice</b>	0.582028118	0.510032	0.488568	0.439858	0.382966
<b>Coated rice</b>	0.582028118	0.512401	0.486414	0.437242	0.382303
<b>Coated/ Medium</b>	0.5913905	0.518422	0.490742	0.444735	0.383632

**Table S1.** *d*-spacing (nm) in each crystalline type of rice grain sample calculated by XRD data

<i>Gene name</i>	<i>No. of peptides (*Sequence Count)</i>	<i>Description</i>
<i>Q3MHM5</i>	<i>10</i>	<i>Tubulin beta-4B chain</i>
<i>O62654</i>	<i>162</i>	<i>Desmin</i>
<i>Q148J6</i>	<i>21</i>	<i>Actin-related protein 2/3 complex subunit 4</i>
<i>F1MH07</i>	<i>21</i>	<i>[F-actin]-monooxygenase MICAL1</i>
<i>A7MB43</i>	<i>12</i>	<i>Myotubularin-related protein 9</i>
<i>A6QLT4</i>	<i>8</i>	<i>Myotubularin</i>
<i>Q28824</i>	<i>9</i>	<i>Myosin light chain kinase, smooth muscle</i>

**Table S2.** Myogenic differentiation-related proteins identified by LC-MS/MS proteomic analysis.

\*Sequence count means the number of peptides identical to the Description and is generally considered reliable data from more than 5.



Cas No.	Compound Name	Flavor description	Peak Area		
			Bare rice	Muscular-rice	Fat-rice
124-19-6	Nonanal	Lemon	10480177	5103105	4316532
1669-44-9	3-octen-2-one	Creamy	-	-	919055
123-96-6	2-octanol	Mushroom	3615039	-	-
66-25-1	Hexanal	Apple	8237208	9103083	7462414
3777-69-3	2-pentyl furan	Butter	-	-	1027010
104-76-7	2-ethyl-1-hexanol	Green	9043700	-	-
124-13-0	Octanal	Citrus	4107623	1949602	2013861
1014-60-4	1,3-bis(1,1-dimethylethyl)benzene	Beef	-	15205013	-
96-76-4	Phenol, 2,4-bis-(1,1-dimethylethyl)	Smoky	-	7357545	-
100-52-7	Benzaldehyde	Almond, Beef	14605490	108996410	2611638
100-51-6	Benzyl alcohol	Bread	3050419	-	-
56-81-5	Glycerine	Coconut oil, Sweet	-	-	4894694

**Table S3.** GC-MS detects odor peaks in raw samples. Volatile compounds from each sample (uncoated rice, muscular-rice, and fat-rice) were detected, and the odor of each volatile

compound was described with reference to the Flavor Extract Manufacturers Association (FEMA) and the Joint FAO/WHO Expert Committee on Food Additives (JECFA).

Pdf by:  
<https://www.pro-memoria.info>